

UC Berkeley

UC Berkeley Previously Published Works

Title

Spatial EEG Patterns, Non-linear Dynamics and Perception: the Neo-Sherringtonian View

Permalink

<https://escholarship.org/uc/item/08d8g56h>

Journal

Brain Research Reviews, 10(1)

Authors

Freeman, Walter J, III
Skarda, Christine A

Publication Date

1985-08-27

Copyright Information

This work is made available under the terms of a Creative Commons Attribution License, available at <https://creativecommons.org/licenses/by/3.0/>

Peer reviewed

BRR 90038

Spatial EEG Patterns, Non-linear Dynamics and Perception: the Neo-Sherringtonian View

WALTER J. FREEMAN and CHRISTINE A. SKARDA

Department of Physiology-Anatomy, University of California, Berkeley, CA 94720 (U.S.A.)

(Accepted August 27th, 1985)

Key words: brain theory — electroencephalogram (EEG) (spatial form) — non-linear dynamics of EEG — olfactory perception — perception — self-organization (EEG studies) — spatial analysis of EEG

CONTENTS

1. Introduction	147
2. Spatial analysis in the olfactory bulb	148
2.1. Prior evidence	148
2.2. Multiunit recording	149
2.3. EEGs from naive animals	150
2.4. EEGs under serial conditioning	152
2.5. EEGs under discriminative conditioning	153
2.6. Analysis of EEG spatial patterns	155
3. Neural dynamics manifested in EEGs	157
3.1. EEG oscillations	157
3.2. The static non-linearity underlying bursts	158
3.3. The commonality of EEG waveform	160
3.4. Odor-specific information in the EEGs	161
3.5. The disorderly bursts: chaos?	163
3.6. Limitations of the approach	164
4. Implications for neurophysiology	165
4.1. Sensory systems and perception	165
4.2. Implications for motor systems and pattern generators	166
4.3. Goal-directed behavior	168
4.4. A retraction on 'representation'	169
5. Summary	171
Acknowledgements	171
Glossary	171
References	172

1. INTRODUCTION

Recent developments in electronics have given access to new dimensions in the study of brain activity. Arrays of preamplifiers make it possible to record si-

multaneously from large numbers of electrodes or optical sensors placed on or in the brain; computers enable reduction and display of the immense quantities of data that rapidly accrue, and they provide the tools for constructing and testing heuristic dynamic

Correspondence: W.J. Freeman, Department of Physiology-Anatomy, University of California, Berkeley, CA 94720, U.S.A.

models of brain systems. As with any new technology such as electrocardiography, X-ray imaging, electron microscopy, tomography and so forth, several years of experimentation are required to explore its possibilities, the kinds of patterns it reveals, and what they might mean. Large series of images are necessary to give observers a sense of familiarity and confidence in what they see or do not see. New subsidiary techniques are needed for electrode design and manufacture, for preparation of animals to give access to recordings, and for data collection and processing. Standardized experiments are required to serve as benchmarks, and rules of evidence or criteria for the validity of data must be formulated. An appropriate nomenclature and convenient set of conventions for graphic display must be agreed upon.

Most importantly, a body of theory must be developed as the basis for correct processing, display, evaluation and interpretation of these new data. Present technology has already let loose a flood of new data and provided sophisticated devices for 2-D display of various facets, but the major problem is to develop some expectations of what the data should reveal. The situation is analogous to that of archeologists faced with an undeciphered written language; only by deducing some underlying rules from the specimens and their functional context can they distinguish meaningful form from adventitious artifact, or 'signal' from 'noise'. For neurophysiologists this means that a curve or a surface, which is the prediction of a model such as the solution of a set of equations, must be fitted to the processed data. The specification is: 'This is what the data ought to look like, if what we believe is valid.' If the agreement is poor, either the belief is changed or the data are processed in a different way. Although non-scientists commonly suppose that disagreement is cause for rejection of a theory, the usual outcome in good science is disclosure of an artifact or deficit in data processing.

This essay contains a review of procedures for collecting and processing multiple electroencephalograms (EEGs) from the olfactory bulb and cortex of the cat and rabbit³⁵, some examples of the data, some theoretical bases for interpreting them, and some of the implications for understanding bulbar function in olfactory perception³², learning⁵ and imprinting⁵¹. These topics are relevant for electroencephalogra-

phic studies of other brain systems and species and for the data accruing from multichannel optical recordings of tissues impregnated with voltage-sensitive optical probes⁴⁹. They will become relevant for spatial analysis of magnetoencephalograms and microelectrode unit activity as technical developments allow use of adequate numbers of channels.

Spatial analysis requires a sufficient number of channels at close enough intervals so that the spatial texture and pattern of activity can be observed in or over a contiguous part of the brain. Description of the receptor field of a single neuron does not qualify, because this does not reveal the spatial activity pattern within the receptor layer or in the nucleus or cortical area to which the neuron belongs. Likewise, the collection of EEGs from selected scalp placements does not qualify; at best this provides a sample for correlation analysis of activities from different brain structures. Some early examples of spatial analysis are the derivation of phase gradients for the alpha rhythm in humans by Walter¹⁰⁷ in 1953, and the display of spontaneous and click-induced waves in the anesthetized cat by Lilly and Cherry⁶⁹ in 1955. Low-resolution spatial images of scalp-recorded EEG activity from humans with 16–32 electrodes are now commonplace¹¹. Summaries of reports on EEG spatial analysis over the past 3 decades and on the underlying volume conductor theory are in several monographs: Plonsey⁸⁹ (Ch. 5), Freeman²⁵ (Ch. 4), Livanov⁷⁰ (Ch. 1), and Nunez⁸⁶ (Ch. 7). Other reviews cover the technical procedures of EEG spatial analysis³⁵ and its implications for philosophy⁹⁷ and artificial intelligence⁷. We interpret our results in the language of non-linear dynamics, but our underlying theory is that of axons, dendrites and synapses developed by Sherrington, culminating in his 1929 conception of the central excitatory state⁹⁶. We label our view 'neo-Sherringtonian' in order to emphasize the emergence of our insights from our investigations of the properties of neurons rather than the properties of our mathematical tools.

2. SPATIAL ANALYSIS IN THE OLFACTORY BULB

2.1. *Prior evidence.* The rationale for undertaking spatial analysis was to test the hypothesis of Adrian² and LeGros Clark⁶⁶ that some aspects of olfactory responses to odors might be spatial. The hypothesis

was based mainly on the structure of the olfactory system, consisting of a sheet of receptors transmitting in parallel to a cortical sheet of neurons in the bulb, and this in turn to other laminar structures comprising the olfactory cortex. By analogy to other sensory systems the sensory quality of a stimulus was thought to be conveyed by the selection of receptors in an array and intensity by the rates of firing on the selected axons. Preliminary results from microelectrode recording of unit activity in the bulb of the anesthetized hedgehog suggested that neurons responding preferentially to certain odors might be spatially segregated.

Substantial evidence has now accrued from several species showing that single neurons at all levels of the olfactory system including the mucosa^{18,55}, bulb^{60,67,73,75}, piriform cortex^{50,84} and orbitofrontal cortex^{81,100} respond selectively to presentation of odorants over relatively narrow ranges of concentration with excitation, concentration specific⁷⁷ or non-specific¹⁵ inhibition, or complex patterns¹⁰⁹ of firing. The specificity of responding is poorly defined, in the sense that each neuron tested tends to respond to multiple odorants⁶⁷. This cross-reactivity holds also at all levels, so that olfactory neurons might be said to be broadly tuned with no evidence for narrower tuning at more central levels. In the terms of Edelman²¹ the 'coding' is 'degenerate' as distinct from 'labelled line'. Despite suggestive evidence from genetics and selective anosmias³ there is no agreement on the numbers of primary odors in olfaction analogous to colors in vision, except that, if they exist at all, and they need not, they might range from³ 20–30 to as many⁶⁶ as 500.

Neurons responding similarly to the same odorant or set of odorants tend not to be homogeneously distributed^{79,82,102} in the olfactory mucosa and bulb. Evidence from recording configurations of locally summed receptor slow potentials in the mucosa⁷² and of retention times of odorants⁸³ also indicates that different odorants establish different spatial patterns of activity in the mucosa. The topographic order that exists in the primary olfactory nerve from the mucosa to the bulb^{25,66} indicates that spatial pattern differences between odorants should exist in the bulb as well. Prolonged exposure to an odorant has led to selective degeneration of mitral and tufted cells¹⁷, that might reflect induced odor-specific activity patterns.

Regional differences in metabolic activity during prolonged odor exposure have been demonstrated with 2-deoxyglucose in the glomerular layer of the bulb^{14,58,64,65,94,98,99}. These latter approaches have not yet had adequate controls done for individual variability; they permit only one odorant for each subject. Nevertheless, the cumulative results lead to the prediction that when two odorants are presented to an animal on randomly interspersed trials, the neural activity induced in the bulb should co-vary between two distinctive spatial patterns that are correlated with the odors. This is not to say that odorant information is 'encoded' in the patterns or that other aspects of the neural activity are unimportant. It is to say that the spatial patterns should exist, and the forms and the conditions in which they are found should be interesting.

Four experiments are described here that were done over the past 12 years. Each yielded some essential insights, that cumulatively led to a coherent picture, although in no case were the results fully consistent with the initial predictions. The conditions in which all of the experiments were done included (a) use of multiple electrodes with simultaneous recordings, (b) chronic implantation with recording after surgery from animals in aroused or motivated states and (c) observation of spatial patterns in time periods corresponding whenever possible to single inhalations without ensemble averaging. These conditions were based on our expectation that the most interesting patterns would be those found in animals that were in near-normal states of behavior and were responding to the odors in a goal-directed manner.

2.2. Multiunit recording. The first experiment²⁵ was done with ten 40-micron wire electrodes attached to a shaft at intervals of 0.1 mm along a line 1 mm in length. The device was inserted with a miniature stereotaxic drive clamped to a stainless steel well previously mounted surgically and filled with agar over the exposed dorsal bulb. The minimally restrained rabbits were deprived of food 24 h before each recording session and fed immediately thereafter. Odorants were presented in solution with a cotton pledget held before the nose to induce exploratory sniffing, after the electrodes were placed from above into the external plexiform layer (EPL) parallel to the mitral cell layer. Ten preamplifiers, high and low pass filters, threshold detectors, and pulse

shapers and 12 oscilloscopes were used to record units and the EEG, along with a pneumograph trace and an EEG trace recorded monopolarly with respect to the nasal bones from a permanent electrode in the bulbar interior. The 22 traces were multiplexed, digitized and stored in core and then on tape.

The results showed that spatially there were marked inhomogeneities in the amounts of unit activity observed in different parts of the bulb. Two regions roughly 2–3 mm across were repeatedly found to have the greatest activity, one in the ventromedial quadrant and the other in the mid-lateral wall of the bulb. No region of the EPL was silent, but minimal activity was found in the dorsal wall. Regular fluctuation with inhalation was the rule; an audiometer gave the sound of surf. Activity broadly increased with episodes of behavioral arousal and exploration, and it decreased with apathy and torpor. No relationships were identified between unit activity and odors.

On the one hand we concluded that the sample from 10 electrodes was far too small to discern the spatial patterns of bulbar activity, and that technical difficulties would preclude adding more channels. On the other hand we observed consistent positive correlations between the amounts of unit activity and the amplitude of the entire spectrum of EEGs (corrected for depth position with respect to the bulbar dipole) in respect to location in the EPL, respiratory fluctuations and changes in motivated behavior. Statistical analysis demonstrated that the firing probabilities of single cells and the relative frequencies of multiple units oscillated at the same peak frequency as the EEG near the same part of the bulb. From our understanding²⁵ of the mechanism by which the EEG was generated we concluded that spatial analysis should be done with the EEG prior to further work with units, in order to define sample spaces for unit analysis.

2.3. EEGs from naive animals. The second experiment^{26,27} was done with prefabricated arrays of electrodes surgically placed epidurally onto the lateral face of the bulb. Two types were used. One was a set of 64 wires, 0.1 mm in diameter along a line 6.4 mm on the surface. The 1-D Fourier transform was done on single measures after linear extrapolation to correct for the digitizing delay (10 μ s/read or 0.64 ms/frame) and on root mean square (rms) amplitudes of

EEG segments 100 ms in duration. A cut-off frequency was identified at 1.0 c/mm above which no spectral peaks occurred²⁶; this was consistent with the spatial passband of the granule cell field potential generator, that was calculated from a volume conductor model. The other type¹⁹ was an 8 \times 8 or 6 \times 10 array of 0.25 mm wires with spacings of 0.5 or 0.8 mm that was guaranteed by data from the linear electrode to minimize aliasing. Recordings were made in the behavioral conditions already described; sets of 64 traces were displayed in rasters with a pen plotter.

The outstanding feature of these sets was the commonality over the array of the EEG wave form. The typical pattern of bulbar traces in aroused animals (Fig. 1) was a slow wave closely related to respiration (surface negative with inhalation) and a burst of oscillation in the gamma range (35–90 Hz in the rabbit) on each crest of the respiratory wave. This pattern was common to all channels. Each burst had the same number of peaks and zero crossings. Hence each burst could be described by its peak frequency from the FFT and by 64 \times 1 matrices of rms amplitude and of phase with respect to the ensemble average phase calculated by time-lagged correlation. In consideration of the observed spectral peak frequencies the

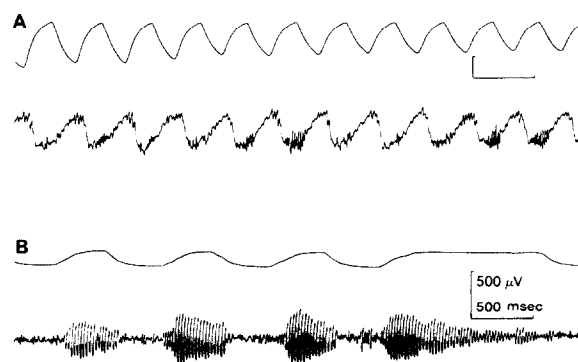
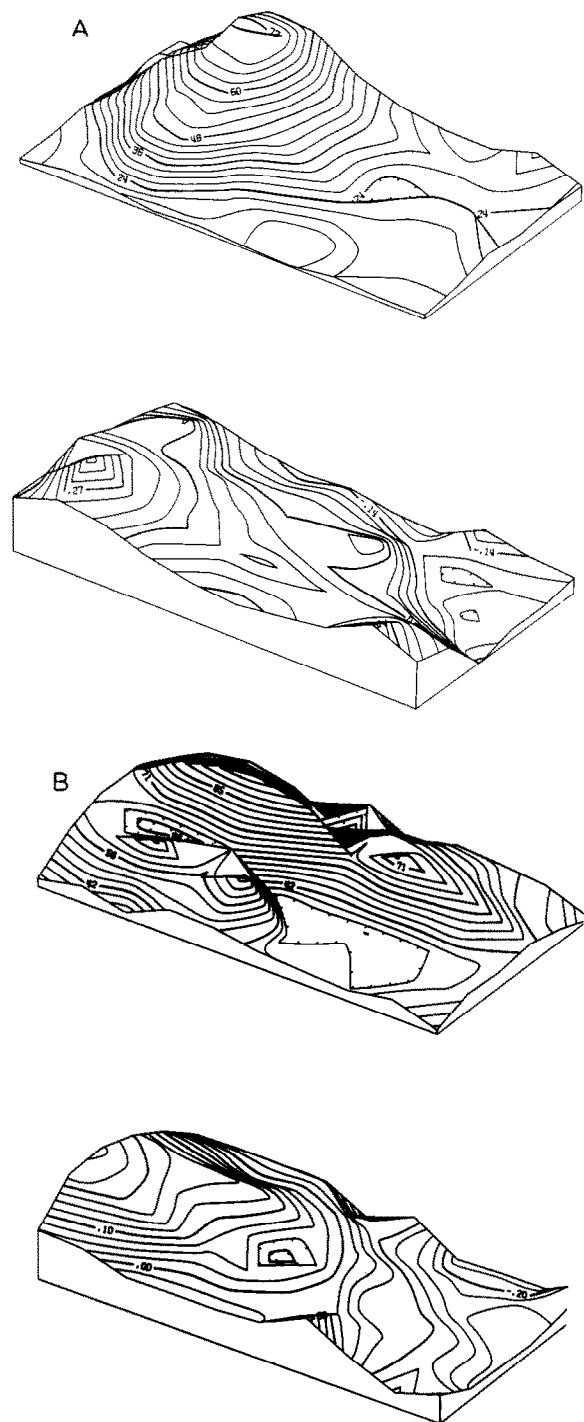


Fig. 1. A: the lower trace shows the EEG from the surface of the olfactory bulb in a hungry rabbit; the upper trace shows respiration measured by a pneumograph. The characteristic EEG pattern is a burst at 60–70 Hz with inhalation (upward) superimposed on a respiratory wave (negative downward). B: the lower trace shows the EEG from the bulbar surface in a cat under light chloralose anesthesia and with a tracheotomy. The upper trace shows the airflow pulled through the nose (deflection upward) with a respirator attached to the distal end of the trachea. The respiratory wave was filtered from the EEG. The bursts depended on air flow and not on centrifugal input to the bulb from the respiratory centers, because the respiratory rate was about twice that shown for the nasal air flow.

temporal digitizing interval was increased from 1 to 2.5 ms. In further off-line editing only the bursts were saved. These steps reduced the data by nearly 2 orders of magnitude and for the first time provided routine spatial overviews. The 8×8 matrices of single frame or rms amplitudes and phases were displayed



by contour plots with second order extrapolation or by density plots, either printed on paper or displayed on an oscilloscope in the form of movies.

We papered the walls of the laboratory with these plots, discovering that each animal had its characteristic spatial patterns of phase and amplitude, that like signatures were easily recognized but never twice identical²⁷ (Fig. 2). Bulbar amplitude patterns took the form of foci with half-amplitude diameters averaging about 2 mm, with irregular borders, and with the centers in or presumably just outside of the array. The 8×8 arrays were always fixed with the posterior edge at the posterior border of the lateral bulb and the anterior edge over the middle third (see Fig. 8). Thus, the EEG foci were located at a position corresponding approximately to one of two locations of intense activity in the bulb identified by unit recording and the 2-deoxyglucose method. These loci, interconnected by associational fibers⁹², also corresponded to regions of small glomeruli, small mitral cells and high neural density analogous to retinal foveae⁷⁸.

The details of the shapes of foci varied erratically and unpredictably, as did the mean rms amplitude from each burst to the next. The bulbar phase pattern took the form of a gradient averaging 0.25 radians/mm with a range of values roughly ± 0.45 radians over the array, but the orientation of the gradient with respect to the array varied randomly around the clock on successive bursts. This contrasted with patterns from the prepyriform cortex, which showed

←

Fig. 2. The upper frames show perspective contour plots in microvolts of the root mean square (rms) amplitude of EEG bursts from 6×10 arrays of 60 electrodes at 0.8 mm spacing (4×7 mm). The lower frames show the plots of phase in radians with respect to the ensemble average. A: plots from a burst at 59 Hz from a hungry cat with the array on the lateral surface of the bulb; anterior is upward and dorsal is to the right. The amplitude pattern was relatively constant across bursts; the location of the phase maximum or minimum and the direction of the phase gradient varied at random across bursts. B: plots from a burst at 65 Hz from a hungry rabbit with the array on the prepyriform cortex and olfactory nucleus; dorsal is upward and posterior is to the right. The lateral olfactory tract ran under the middle of the array parallel to the long edge from left to right. The phase gradient was consistent with the 5 m/s conduction velocity of this main segment of the tract and with the 2 m/s velocity of the terminal segments to either side. The maximal amplitudes occurred on both sides of the tract at locations that were relatively stable²⁷ unless the animals were conditioned.

multiple peaks of amplitude like islands eccentric to the lateral olfactory tract (LOT) and a phase gradient consistently in the direction of the LOT, that was compatible with its conduction velocity (from 5 down to 2 m/s in these segments).

Up to 24 odorants were presented to each animal, and odor bursts were recorded, processed and compared with control bursts. In no instance were consistent differences either in phase or in amplitude found to depend on odorants. The amounts of difference between control and test odor bursts did not exceed the differences between pairs of control bursts, although the animals were commonly observed to sniff to the odorants.

2.4. EEGs under serial conditioning. Previous studies of olfactory EEGs repeatedly showed that the major behavioral correlates were between EEG amplitudes and the levels of arousal, motivation and attention²⁵. We inferred that detection of an EEG pattern difference with an odorant might require us to

train animals to respond to the odorant. Also, we wished to control for possible selective anosmias. In the third experiment³⁹ we used classical aversive conditioning by pairing each presentation of an odorant as a conditioned stimulus (CS+) with a brief electric shock to the paw or cheek (UCS). The odorant was delivered with a dilution olfactometer⁸⁰ and automated solenoid valves into a steady air stream for 3 s, with the UCS given 2.5 s after odor onset. The conditioned response (CR) was measured by the rate of occurrence of sniffing over sets of 10 trials relative to background sniff rate. While not entirely conventional, this autoshaped response had the advantage of becoming clearly established well within 10 trials in a session^{16,41}, as compared with other CRs such as paw flexion and nictitating membrane retraction that took several sessions to reach criterion. Rapid learning was urgently needed in order to minimize the quantity of EEG data.

In the first session with each of 6 rabbits a differ-

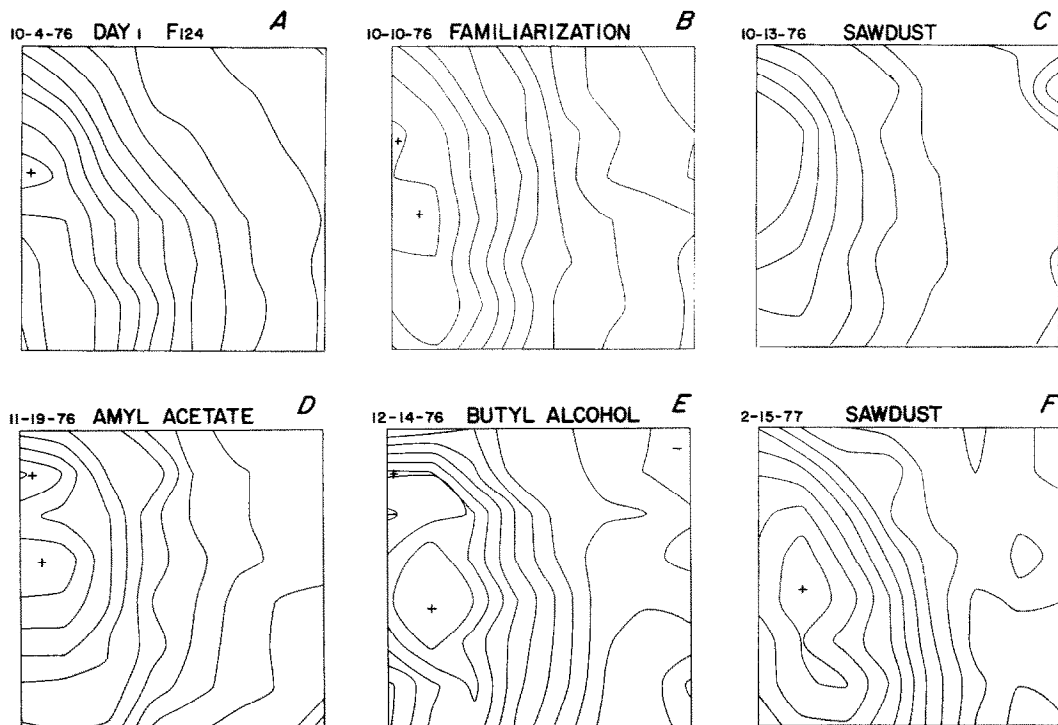


Fig. 3. The contour plots are shown for the mean EEG rms burst amplitude from a trained rabbit over a period of 4 months. In main outline the focus was sufficiently stable to serve as the 'signature' pattern characteristic of this animal. Without conditioning such patterns remained unchanged for months. Under aversive or appetitive conditioning they changed with each new set of stimulus-response contingencies. Examples are shown of 5 such changes with classical aversive conditioning as well as familiarization to the recording apparatus. Presentation in the last stage of the odorant 'sawdust' used in the first stage did not result in return to the EEG pattern of the first stage³⁹.

ence was found in the spatial pattern of amplitude between the contour plots of the ensemble averages of odor bursts and the control bursts preceding them. These differences did not appear to be statistically significant under Hotelling's T^2 , linear discriminants, or various types of cluster analysis. An empirical test emphasizing the tails of the distributions was devised, which consisted of computing the 64 t -values for the channel mean differences between 10 control and 10 odor bursts, and calculating a χ^2 value for the experimental t -distribution against Student's t -distribution. Control-control t -distributions were found to conform to the latter. The distribution of χ^2 values was formed for 1180 control-control comparisons from 11,800 pairs of control bursts, and a 97.5% upper limit was defined. Then any control-odor comparison exceeding that limit (e.g. $\chi^2 = 100$) was inferred to reflect a significant difference for that session, CS+ odorant, and animal (Fig. 3).

The pattern differences were significant for all animals in the first session, but by the third session they were not. The spatial patterns had evolved to new forms with return to the previous low levels of variance. A new CS+ was presented in the 4th session, and again in the 7th, each time with emergence of a significant difference followed by re-stabilization of a new pattern by the 6th and 9th sessions. Return in the 10th session to the CS+ used in the first session gave another replication with appearance of a new pattern and not the pattern seen with the same CS+ in the first session. The pattern changes did not accompany repeated odorant presentations without reinforcement (CS-) nor presentations of the UCS paired with visual and auditory CS+s.

These results showed that expectancy and its modification by learning played a role in bulbar EEG pattern formation for odor CS+s. They left unanswered the questions how the pattern might differ depending on the presence or absence of the odorant (clearly the animals detected the CS+ odorant, usually in a single inhalation, even though the control and odor bursts did not differ significantly), how an unexpected odorant leading to behavioral responses might affect bulbar patterns, and how expectations of two or more odorants might be reflected in bulbar activity patterns.

2.5. *EEGs under discriminative conditioning.* In the fourth experiment¹⁰⁵ we used classical appetitive

conditioning by depriving rabbits of water for 24 h, pairing 1 ml of water with an odor CS+ and not with an odor CS- on randomly interspersed trials, and measuring both the sniff CR- (to the CS-) and the jaw movement CR+ (to the CS+) as a part of the licking response detected electromyographically. The hypotheses were tested that (a) between the times of onset of the sniff signifying detection of an odorant and of the CR+ (if any), odor-specific information existed in the bulb as the basis for decision, (b) that this information would be detectable as a difference in spatiotemporal patterns between bursts with the CS+ and CS- odorants and (c) that both patterns would differ from a pattern C+ and C- characterizing a homogeneous control state preceding the odorants. The test was to measure the bursts and to use the numbers to classify bursts in respect to stimulus condition. A positive outcome would be correct classification of CS+ and CS- bursts above chance levels and not of C+ and C- bursts. Initially, the test was restricted to trials on which correct CR+ and CR- responses had occurred and to the 4 of the 5 subjects that showed significant behavioral evidence for odorant discrimination. The data were taken from the 4th-6th session for development of the measurement and classification procedures.

The matrices of rms amplitudes sufficed to distinguish control from odor bursts but not CS+ from CS- bursts. More accurate measurements were made by fitting curves to the 64 traces of each burst. The technique was (a) to form the ensemble time average of the 64 traces, (b) to calculate its spectrum with the FFT, (c) to make initial guesses of the frequency and phase of a cosine from measurements on the peak of the spectrum, (d) to fit the cosine to the ensemble time average using non-linear regression^{25,36}, (e) to optimize estimates of the amplitude, frequency and phase of a cosine both amplitude- and frequency-modulated linearly over time, (f) to subtract the fitted curve from the data and (g) to repeat the process 4 times. The sum of these 5 fitted curves incorporated 97% of the variance of the ensemble average. Then (h) the frequency and the modulation parameters were fixed, and the amplitude and phase were determined by regression for each of the 64 traces. This incorporated about 80% of the variance of the bursts. Thereby the 64 EEGs of each burst were decomposed into parts^{35,40}.

As in a chemical separation procedure, all of the parts (the amplitude and phase matrices, the set of frequency measurements, and the matrices of residuals) were tested in turn for efficacy in classification. The simplest effective test for each set of matrices was to calculate in 64-space a centroid for the C+, C-, CS+ and CS- bursts, to classify as 'correct' each CS+ and CS- burst for which the Euclidean distance from its point in 64-space to its own centroid $\overline{CS+}$ or $\overline{CS-}$ was shorter than to that opposing, similarly to classify the C+ and C- bursts with respect to the $\overline{C+}$ and $\overline{C-}$ centroids, and then to subtract the % 'correct' control bursts from the % 'correct' odor bursts. This percentage difference measure served as a 'touchstone' to locate odor-specific information and to optimize the following 4 procedures for its extraction.

Systematic testing showed that the only fraction containing odor-specific information was the matrix

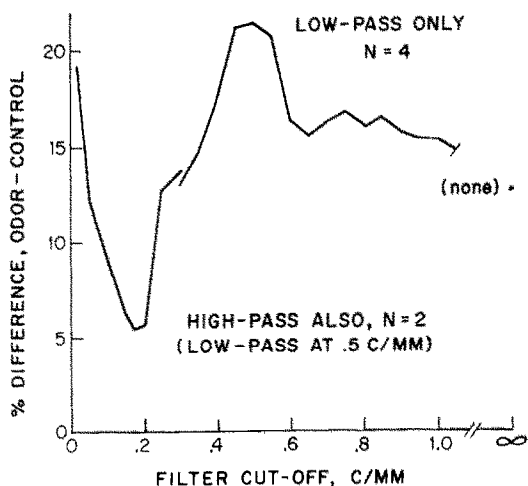


Fig. 4. The ordinate shows the classification efficacy of a Euclidean distance measure (see text) applied to a total of 418 bursts from 4 rabbits trained to discriminate a CS+ from a CS- odorant. It is expressed as the difference between the percentage of odor bursts correctly classified with EEG measurements minus the percentage of control bursts 'correctly' classified (e.g. 76%–55%) on the premiss that control bursts C+ and C- from pre-stimulus intervals were not significantly different. The abscissa shows the cut-off frequency (3 dB fall-off) of a 2-D spatial N-th order exponential filter applied to the amplitude matrices of the dominant EEG components in the spatial frequency domain. The data at the right show that removing high spatial frequencies improved the classification rate with the optimal cut-off frequency between 0.4 and 0.5 c/mm. The data at the right show that the odor-specific information was maximally removed from the EEG with a high pass filter as well set at 0.17 c/mm. This spatial frequency lay in the EEG passband of the granule cells^{31,35,37,40}. C/MM, cycles/mm.

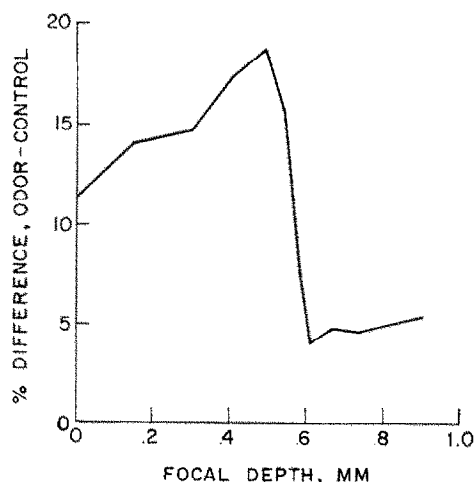


Fig. 5. Spatial deconvolution of the EEG acts as a 'software lens' to compensate for the blurring effect of the volume conductor on the neural activity pattern as it is manifested in the surface EEG pattern. For a dipole field with its zero isopotential surface parallel to the bulbar surface the optimal depth of focus should correspond to the depth of the zero isopotential ('turnover'). In the anesthetized bulb this lay about 0.1 mm above the depth of the mitral cell layer^{25,91} (ca. 0.6–0.7 mm in the posterior bulb of the rabbit). The optimal depth of focus by the correct classification criterion was 0.49–0.54 mm. Use of this procedure requires prior use of low-pass spatial filtering to remove activity from a more superficial dipole in the bulb⁷⁶, electrode noise, and possible other contributions to the EEG not from granule cells. The procedure removes the contribution to the EEG from the monopolar reference electrode^{31,35,37,40}.

of amplitudes of the largest or dominant component of the bursts, comprising on the average about 50% of the total variance of the 64 EEG traces. Several procedures were found to improve classification efficacy. One was to apply a low pass spatial filter that was designed to conform to the passband of the granule cells and to remove contributions to the EEG from other sources⁷⁶. The filtering was done in the spatial frequency domain⁴⁴ by use of the forward and inverse 2-D FFT without Hamming and a 2-D 4th-order exponential filter. Repeated calculation of the touchstone (Fig. 4) over a range of values showed that the optimal cut-off frequency was 0.5 c/mm, and that a minimal touchstone value obtained with a high pass spatial filter set at 0.17 c/mm, thereby attenuating activity at the center of the array passband.

A second procedure was spatial deconvolution^{31,35}. The actual spatial activity pattern of granule cells was distorted in its manifestation in the surface EEG in a manner that resembled blurring out of fo-

cus of an optical image. The 'point spread function' of the blurring was known from volume conduction studies of the bulb^{25,26,34,37,91}. Deconvolution (the 'software lens') served to re-focus the patterns. Values of the touchstone for a range of focal depths yielded a tuning curve^{37,40} with an optimal focal depth at 0.49 mm (Fig. 5), approximately 0.1–0.2 mm above the depth of the mitral cell layer determined post-mortem in these animals.

A third procedure was channel normalization. Over an entire set of bursts to be classified (e.g. 360 for each animal) the mean and standard deviation (SD) were calculated for each channel, and the data were expressed as z-scores (zero mean and unit SD). This effectively removed the 'signature' pattern of the amplitude focus from the data of each animal and equalized the variances of the contributions of the 64 channels³⁶.

A 4th procedure, the most effective and important, was prior classification by temporal frequency^{35,36}. The temporal spectrum by the FFT of most bursts had a high, narrow peak between 55 and 75 Hz, but 20% of control bursts and nearly 50% of test bursts had a maximal peak below 55 Hz. These lower frequency bursts tended to have broad spectra with multiple peaks and large frequency modulation in the time domain. Spatially also they were less coherent. Whereas the correlation coefficients of the 64 amplitudes of sets of control, CS+ and CS- odor higher frequency bursts averaged in excess of 0.8, those between lower frequency bursts averaged less than 0.2. Bursts with peak frequencies less than 55 Hz and with FM exceeding 50% of the center frequency were labelled 'disorderly' or 'chaotic'. They did not contain odor-specific information and were deleted (Fig. 6).

2.6. Analysis of EEG spatial patterns. Amplitude matrices that were selected and transformed by these procedures were further transformed by factor analysis^{35,38,40} into the coordinates of the principal components of the variance. From 4 to 11 factors incorporated 88–96% of the variance. The odor-specific information was converted to factor scores on the factor loadings. Linear discriminant analysis of the factor scores confirmed the validity of the touchstone, and demonstrated 74–100% correct classification of bursts. The analysis was readily extended to trials on which no or incorrect responses had occurred, with lower but still significant ($P < 0.01$ for each animal)

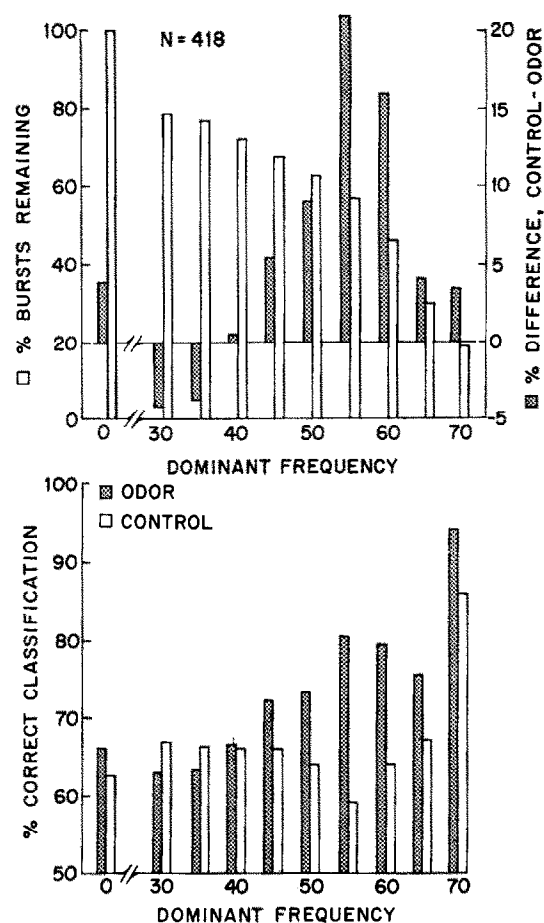


Fig. 6. A finding of major importance was the fact that about 20% of control bursts and 48% of odor bursts do not fall into reproducible categories of spatial amplitude pattern. When they are included in discriminant analysis, they violate the assumption of equal variances among groups and obscure the order that does exist. The key property by which to 'label' these disorderly bursts is their peak frequency in the time domain. The upper graph shows that optimal classification is achieved when bursts with peak frequencies less than 55 Hz are removed before classification. The lower graph shows that when the disorderly bursts are not excluded, or when group sizes become too small, the rate of 'correct' classification of control bursts C+ and C- becomes too high^{35,36,40}.

classification rates. Each data set served successfully as a 'test' set for cross-classification from the coordinates determined by a 'learning' set. The EEGs from a rabbit that failed behaviorally to discriminate the CS+ and CS- odor in these sessions served to classify correctly odor from control bursts but not CS+ from CS- bursts. Finally, the bursts from each of the 3 sessions irrespective of CR were transformed by factor analysis; each set of factor loadings served to gener-

ate factor scores on the same ('learning') and the other ('test') sets. Classification rates ranged from 58 to 83% correct with no significant differences between test and learning sets. The stability of the factor patterns over the 3 sessions was further demonstrated by cross-correlation of the 3 sets of factor loadings^{35,38,40}. Comparable classification results were obtained with alternative statistical procedures⁴⁶.

The data so far described were taken from 3 sessions out of a total of 18 sessions¹⁰⁵. Training was in 3 stages of 6 sessions each: odors A+ (reinforced with water) and B- (not reinforced); odors C+ and B-; and odors C+ and A- (reintroduced without reinforcement). The procedures for curve-fitting, filtering, transformation and selection were applied to the data from 5 subjects and all sessions. The classification rates ranged from 58 to 86% correct, averaging 73%, all far above chance levels (33%) for each subject and session. Cross-correlation of factor loadings revealed factorial invariance within each stage, but sharp breaks between stages at which the S-R contingencies were changed, and at which the factor patterns changed. These breaks corresponded to changes in spatial patterns of rms amplitude that had been shown to occur in the same manner as with spatial pattern evaluation under serial³⁹ and discriminant¹⁰⁵ conditioning.

These results established the fact that the matrix of amplitudes of the dominant oscillatory component carried odor-specific information. The next question was on which channels. An answer was found by calculating the touchstone value for the sets of bursts from the 4th to 6th sessions of Stage I as before, but deleting 8 channels, then 16, and so forth until only 8 remained. For each number of channels the test was repeated 40 times while a different set of channels was randomly chosen for deletion. After each test an entry was made for each channel used into an 8 × 8 table of the touchstone value resulting. The sum of touchstone values for each channel was divided by the number of times it was used. The channels that were particularly important or unimportant for classification were expected to have mean touchstone values differing from the grand mean over all channels. The entire procedure was repeated on data with and without channel normalization. The results showed that the channel means were normally distributed, and that the average deviation was less than

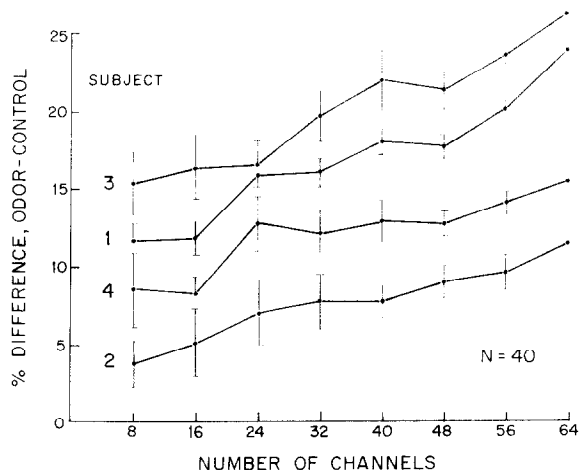


Fig. 7. Channels were selected by a random number generator and their values removed in groups of 8 prior to use of the classification assay. The procedure was repeated 40 times for each rabbit and each number of remaining channels. The means (\pm S.E.M.) for classification efficacy decreased monotonically with the number of channels remaining. Further testing (see text) showed that the odor-specific information was spatially uniform. The level of the classification assay that was significantly above zero ($P < 0.01$) for each subject was 10.3%; by this criterion two subjects showed significant classification with as few as 8 channels, but only on the average by random selection from the 64 channels.

5% of the grand mean ($\pm 0.5\%$ difference from a grand mean touchstone value of 10.6%). For all animals the classification efficacy decreased steadily with decreasing numbers of channels used (Fig. 7). The results implied that the odor-specific information density was uniform among channels across the array, albeit not necessarily in the bulb at inaccessible spatial frequencies. They terminated 12 years of unsuccessful attempts to correlate features of activity on particular electrodes with the presence of particular odorants.

The 8 × 8 array constituted a window covering about 20% of the bulbar surface area and did not impose a boundary. Concomitant surface and depth recordings²⁵ from multiple electrodes⁹ demonstrated commonality of wave form in the EEG in all parts of the main bulb, whenever it was examined in this regard. The spatial extent of coherence far exceeded the spatial range that could be accounted for by volume conduction alone. Application of the new measurement techniques to the low-amplitude and seemingly random activity between bursts showed that the same commonality held between as well as within bursts; that is, the bulb had a common active state at

all times, at least in the waking condition.

Further evidence came from more precise measurements of the bulbar phase gradients (e.g. Fig. 2). On reduction of the error of measurement on single channels in each burst to 0.15 radians (8.5°) it became clear that the gradient was not planar but was conic; that is, the isophase contours formed concentric circles about a point of maximal or minimal phase for each burst. The locations of the extrema were determined by fitting with non-linear regression a cone to the data in spherical coordinates with a radius of 2.5 mm. The fitted surface incorporated on the average 65% of the variance. The conduction velocity of the wave front across the array was estimated for each burst from the ratio of the burst frequency in radians/s (2π times frequency in Hz) to the gradient in radians/mm. The average for the 5 rabbits was 1.73 ± 0.42 m/s. Maxima and minima were about equally likely to occur in both control and odor bursts. The extrema were scattered apparently at random when projected from the sphere onto the bulbar surface (Fig. 8), except that very seldom ($< 3\%$ of bursts) were they projected into the posterior quadrant constituting the bulbar stalk. There was no dependence of location or sign of the extrema on stimulus condition³⁷.

These properties held for both the coherent and the disorderly bursts without significant differences. When the phase values were calculated independently for both the dominant and the secondary components of coherent bursts and were fitted with cones, the extrema of the two components tended to be located near each other. The signs of the extrema agreed in 95.3% of bursts. The correlation coefficients of the surface coordinates for pairs of extrema averaged 0.79. The mean distance between dominant and secondary extrema was 0.80 mm. Assuming that the two extrema were generated by a common process, that is, that they should have been identical in location, the standard error of measurement was ± 0.28 mm. This was about half the mean interelectrode distance of the arrays. The same results held for disorderly bursts but with slightly greater error (± 0.32 mm).

3. NEURAL DYNAMICS MANIFESTED IN EEGs

3.1. EEG oscillations. The salient phenomena to

be explained are the oscillations in the gamma range, the bursts with inhalations, the commonality of waveform over the bulb, the formation of reproducible amplitude patterns in respect to odorants, and the non-reproducible patterns between bursts and in disorderly bursts at lower frequencies. The essential mechanism is provided by the mitral (excitatory) and granule (inhibitory) cells that are coupled by dendrodendritic reciprocal synapses⁹¹ into a negative feedback relation.

Demonstration of this relation is afforded by orthodromic or antidromic electrical stimulation of the bulb at low intensity, such that the response amplitude does not greatly exceed that of the ambient EEG²⁵. The low-level averaged evoked potential recorded at the bulbar surface closely resembles a

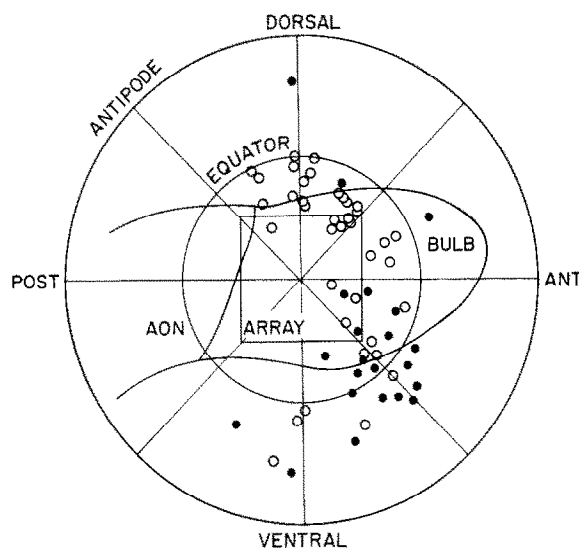


Fig. 8. The left bulb is shown in outline as if viewed from the right side of the head; the rectangle is the outline of the array in its typical location as if seen at its face placed onto the bulb. The rabbit bulb can be approximated as a sphere 2.5 mm in radius. For display purposes the surface of the sphere is presented as a planar surface bounded by a circle at the antipode and centered on the array. The phase pattern of each burst was fitted with a cone in the spherical coordinates so as to capture its pattern of concentric phase contours on the bulbar surface (see Fig. 2A lower part). Distance and angle from the array center to the apex of the cone were used to plot a point in the plane for each burst. It is shown as a solid dot for a phase maximum or as an open dot for a minimum. Both sets of points were randomly scattered over the bulbar surface without regard to odor condition. They were seldom projected into the posterior quadrant where the bulbar surface did not exist⁹¹, those few being regarded as erroneous. The diameter of the open dots is about half the estimated standard error of measurement of the locations of the phase extrema.

damped cosine with an initially negative peak; the field of current is generated by the dendrites of the granule cells and manifests their alternating excitation and inhibition. Post-stimulus time histograms from neurons in the mitral cell layer likewise conform to a damped cosine at the same frequency and negative decay rate but with a quarter cycle phase lead. On impulse excitation the mitral cells excite the granule cells, are inhibited by them, disexcite the granule cells, and are disinhibited by them. Provided there is a pre-existing level of background activity they are re-excited and another cycle begins. If the stimulus intensity is excessive, the background activity is suppressed and only the first cycle remains as a 'diphasic' evoked potential, easily recorded without averaging. Anesthetics of all kinds also reduce the background activity and thereby truncate the response.

Under very deep anesthesia transmission around the loop is blocked. Measurement of evoked potentials in the open loop state gives the open loop time constants of the component neurons. Both the mitral and granule cells have passive membrane time constants averaging about 5 ms. The 4 stages of transmission around the loop for each cycle give a duration of 20 ms and a frequency of 50 Hz. The cycle duration also depends on other factors including the strengths of the synaptic actions that determine the feedback gain, so that oscillation can occur at frequencies in a range from 35 to 90 Hz.

The decay rate of evoked potentials is also determined by several factors, of which the most important is the negative feedback gain. If in a waking animal the stimulus is repeated so as to induce habituation, the response decays more rapidly than at first, implying a more negative decay rate and decreased gain. If the animal is trained to respond behaviorally to the electrical stimulus, the oscillation persists longer, implying that the decay rate is less negative, and the gain is increased. By extrapolation, if factors in attention increase the gain sufficiently, the decay rate may go to zero or become positive, and a stimulus may evoke an undamped oscillation. This phenomenon cannot be demonstrated with the averaged evoked potential technique, mainly because of the destructive effects of averaging over responses with varying frequency, but the concept can be used to explain the EEG burst with inhalation.

These oscillations are the property of populations

of neurons and cannot be explained by entrainment of single neurons^{25,57,88,101}. Median firing rate of the bulbar neurons is 10 pulses/s or less, so that each neuron may fire on the average only once in many cycles. Their pulse interval histograms conform to that of a Poisson process with a brief dead time (the refractory period). Their autocorrelograms seldom show oscillation at the EEG frequency owing to the low pulse rates, and their cross-correlograms have vanishingly small shared power. However, statistical averages over relatively long time periods show that the probability of firing of single neurons in the bulb oscillates at the frequency of the bulbar EEG²⁵.

The demonstration requires digitizing at 1 m/s intervals the EEG from a surface electrode and the pulse train of an underlying mitral cell for 5–15 min, the duration depending inversely on the mean pulse rate (shorter times also with multi-unit recordings). An amplitude histogram (which is almost always nearly normal) is formed of the EEG values in bins arranged in steps of 0.1 SD from -3 to $+3$ SD. A second table for pulses is arranged in two dimensions, one for EEG amplitude and the other for time in 1 ms intervals from -25 to $+25$ ms. For each EEG value (e.g. 60,000 in 10 min) a unit is entered into the table whenever a pulse occurs within the time bin. The number of pulses in each time bin is divided by the number of occurrences of the EEG amplitude, in order to calculate the pulse probability conditional on time and EEG amplitude. The time average over the 2-D table between $+2$ and $+3$ SD of amplitude manifests the pulse probability wave. The ensemble average along the amplitude axis at the times of the upward peaks of the pulse probability wave yields the dependence of pulse probability on EEG amplitude. This experimental relation conforms to a monotonic sigmoid curve that is crucial for EEG analysis (Fig. 9).

3.2. *The static non-linearity underlying bursts.* The bulbar neural mechanism is inherently non-linear. The simplest demonstration is to compare two averaged evoked potentials at different stimulus intensities. Outside of a low-amplitude near-linear range, the larger response to the stronger stimulus has a lower frequency of oscillation. In the population of coupled neurons there are multiple non-linear transformations around the loop, but each has a near-linear range, and most are kept near-linear by the limi-

tation on activity imposed by the most restrictive or dominant non-linearity. This is found at the trigger zones where dendritic current intensity is transformed to pulse firing rate. Over a narrow range in the resting or background state the pulse rate is proportional to the current amplitude, as measured by the potential difference it causes in passing through the extracellular resistance. With increasing inhibition the neurons are suppressed below threshold, so that pulse rate saturates at zero, and further inhibition is not expressed in the output. Similarly, with increasing activity under excitation, the density of activity of neurons in the population approaches a maximum that is determined not merely by pulse-induced refractory periods but, in the long term, by the time needed for recovery, and by long-lasting post-impulse conductance changes.

The slope of the sigmoid curve, which is the rate of change in axonal output with increment in dendritic input, gives the forward gain of this stage of each population. The product of the forward gains around the loop determines the feedback gain. Close examination of the experimental curves shows that the maximal gain does not occur in the resting state. It is displaced to the excitatory side. This means that an excitatory input to the bulb, such as the receptors deliver during inhalation, not only activates the mitral cells and then the granule cells, it increases their feedback gain. The result is the onset of an oscillatory burst that abates during exhalation. A single shock does not suffice, because the activity it evokes does not last long enough. The requirement is for a surge of axonal input that lasts for tens of milliseconds.

The experimental sigmoid relation has been closely fitted with a double exponential curve derived from two opposing membrane-dependent processes²⁸. On the one hand with increasing membrane depolarization there is an exponential increase in likelihood of firing determined by the voltage-dependent sodium conductance. On the other hand the actual expression of that likelihood in the occurrence of pulses is constrained to a maximal rate that can only be approached asymptotically. Examples of these curves and their derivatives, the non-linear gains, are shown in Fig. 9. These properties are quite general; we predict that they will be found to hold for neural populations throughout the brain. The shape of the curve holds for all non-zero levels of background ac-

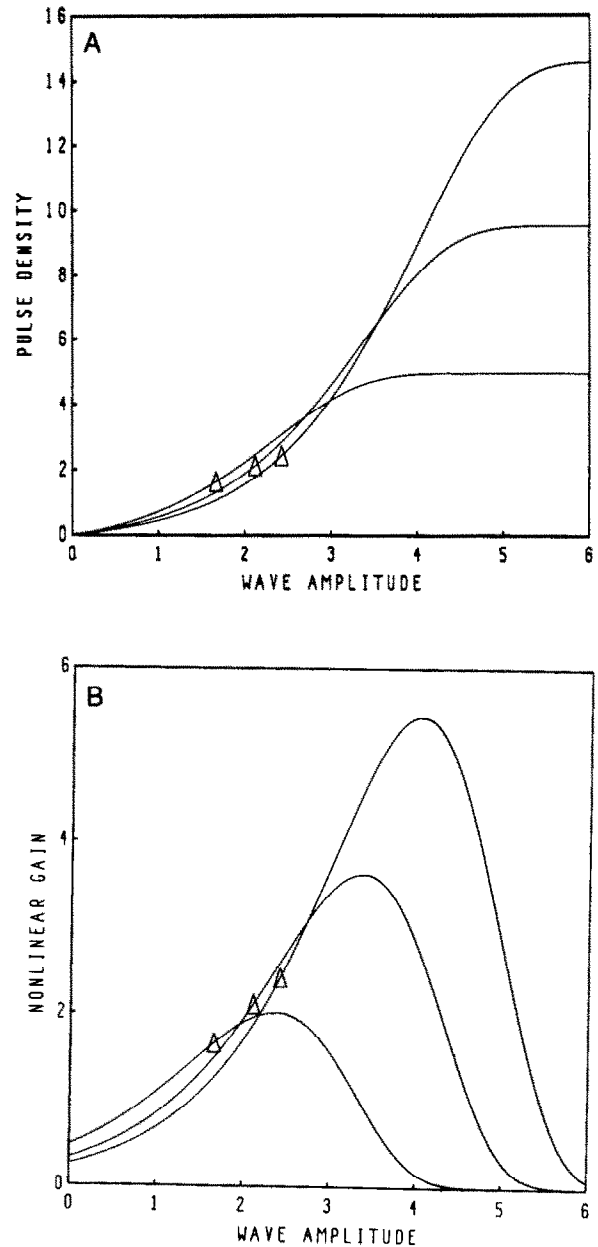


Fig. 9. The static non-linearity of the bulb is determined experimentally from the pulse probability of single mitral cells and small groups conditional on EEG time and amplitude²⁵. The sigmoid curves in A are derived from a mathematical model that related axonal pulse density in a mass to the intensity of dendritic current²⁸. B: the derivative of each curve gives the non-linear gain. The triangles show the mean background values for zero normalized dendritic current amplitude and mean background pulse density. Three examples are shown of increasing an excitatory bias that reflects the level occurring with arousal under centrifugal control. The maximal gain is to the excitatory side of the background level, so that excitatory input from receptors causes a parametric increase in gain in the bulb. This increase underlies the occurrence of the burst.

tivity. Any increase in the background is accompanied by corresponding increases in depolarizing current and in the maximal pulse rate. All 3 variables in the equation for the curves are determined with subsidiary equations from one coefficient that specifies an excitatory operating bias. This bias in the bulb is under centrifugal control by processes relating to arousal or motivation; provisional pharmacological evidence suggests that it is mediated by the centrifugal cholinergic projection to the bulb⁹³. The significance of the depolarizing bias for control of negative feedback gain is reflected in the fact that bursts occur in the bulbar EEG only in aroused or motivated animals, and the burst amplitude is directly proportional on the average to the degree of motivation as measured by the duration of food deprivation²⁵, the rate of work done by animals for food²⁴, etc.

3.3. *The commonality of EEG waveform.* The neurons in the bulb are arranged in a sheet (Fig. 10) that forms the wall of what Rall and Shepherd⁹¹ have called a 'punctured sphere'. The basal dendrites of the mitral (here including tufted) cells ramify in all directions parallel to the surface for distances in excess of 1 mm from each cell body, forming with their branches a dense feltwork. The dendritic arbors of

granule cells thrust through it toward the surface while making bidirectional synaptic contacts with mitral cells. The input of axons, one each from the 40 million receptors to each bulb in the rabbit, is in parallel to the apical dendrites of the mitral cells. The output is also in parallel by the axons of the roughly 150,000 mitral cells. The input is segregated spatially into encapsulated nests called glomeruli, which form the bulbar equivalent of cortical columns, numbering about 2000 in the rabbit with a mean center-to-center distance of 0.25 mm. The roughly 75 mitral and tufted cells with terminals in each glomerulus and the attendant 30,000 granule cells together comprise a subpopulation that behaves as a neural oscillator. The mitral cells are synaptically coupled with each other by excitatory axosomatic synapses⁸⁵ that are also bidirectional¹⁰⁶. Simulation studies of the stability properties of a model^{29,45} indicate that the granule cells must also interact by mutual inhibition (akin to the network of the eye of *Limulus*), but the mechanism remains unclear. It is possible that this link is provided by bulbar stellate neurons (the cells of Golgi, Cajal and Blanes), which are equal in size and number to the mitral cells, but about which little else is known. Hence, the bulbar mechanism can be represented by a surface array of non-linear oscillators that are coupled both by mutual excitation and mutual inhibition. So also can the prepyriform cortical mechanism²⁵.

A dynamic model of the bulb has been embodied in 64 coupled sets of differential equations that incorporate the static non-linearity³⁰. The several coefficients in the model that represent time, space and gain parameters have been evaluated physiologically by comparing various numerical solutions of the equations with impulse input to data in the forms of averaged evoked potentials and poststimulus time histograms. For a surge of input patterned after the density of receptor input to the bulb during inhalation the model generates a burst of oscillation having the center frequency in the range characteristic of the EEG and with comparable modulation in amplitude and frequency. Owing to cross-linkages between oscillators in the model all elements share the common wave form, no matter how complex it might appear. This result implies that the synaptic linkages among mitral and putatively among granule cells are likewise responsible for the widespread temporal co-

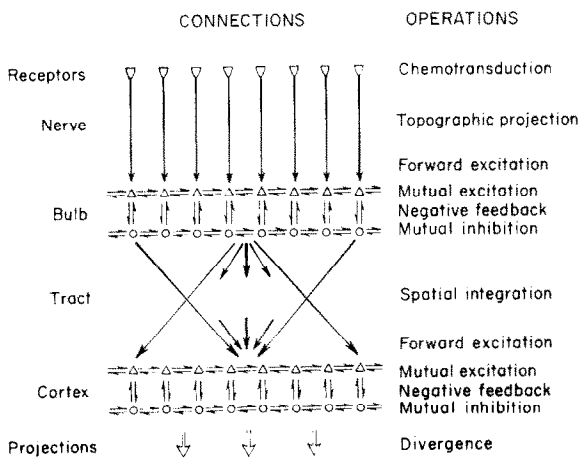


Fig. 10. The first 3 stages of the olfactory system (mucosa, bulb and prepyriform cortex) are shown in outline form, together with phrases to describe the neural operations being done in each stage. The small triangles and circles represent local subsets of respectively excitatory and inhibitory neurons. The arrows represent synaptic transmission³⁴. The hypothesis is suggested in Section 4.2 that the prepyriform cortex might function as a motor cortex; that is, the correlates of its neural activity might appear more clearly in respect to responses than to odorant stimuli.

herence of macroscopic bulbar activity. Certainly the activity in the gamma range cannot be attributed to synchronized input from receptors, because they lack mechanisms for coordination of their firing at the requisite time intervals, and the variations in conduction velocity and distance of their axons serve to smooth out high frequency fluctuations. Only the low frequency respiratory wave is passed, this being controlled by the brainstem respiratory centers through nasal air flow. Bulbar oscillations clearly persist after section of the bulbar stalk and even *in vitro*, so that centrifugal driving cannot explain the commonality. It is a property of the bulb and not of an extrinsic pacemaker²⁵.

Study of the non-linear dynamics of coupled oscillators is a field still in its infancy, but some general concepts have emerged that are helpful in explaining bulbar dynamics^{1,42,53}. A coupled network of realistic numbers (e.g. 64 elements) has an indefinite number of states, but for certain reasonable parameter ranges it displays a manageable number of preferred patterns of activity. Each pattern manifests a dynamic property of the system known as an attractor. Its existence is demonstrated by repeatedly perturbing the system with different inputs and showing that the system returns to one of its preferred states. The domain of input over which this return takes place defines a basin for the attractor.

Three classes of attractors are defined by the character of the preferred activity. If it is rest with steady state or no activity, the attractor is a point reflecting an equilibrium. This occurs for the bulb only under deep anesthesia (the open loop state) or in death. If the activity is periodic, for example, a cosine or any repeating pattern decomposable into a reasonable number of cosines, the attractor is a limit cycle*. The bulb is capable of indefinitely sustained periodic oscillation in certain conditions, such as poisoning by picrotoxin or nicotine, but at abnormally low frequencies. We postulate that bursts manifest the asymptotic convergence to a limit cycle attractor during inhalation, which is aborted during exhalation.

The third type is the chaotic or 'strange' attractor. Its manifestation is activity that appears to be random, but which is deterministic and reproducible if the input and initial conditions can be replicated. Its dimensionality is less than that of random 'noise', although it is difficult to distinguish chaos from an equilibrium that is perturbed by 'noise'³⁵. We propose the hypothesis that the background or interburst activity of the bulb manifests a chaotic attractor in the mechanism. We suggest that the activity arises because the interaction strength of mutual excitation among mitral cells is sufficiently high to sustain regenerative activity; the normalized feedback gain exceeds unity, so that continually their activity tends to blow up. However, they are coupled to inhibitory neurons that dampen their activity and keep it within bounds. A restless and experimentally unpredictable fluctuation emerges at a low amplitude. Most importantly, it is phase-locked over the whole array.

Transition from one attractor to another is called a state change or bifurcation^{1,53}. A change in a parameter is required. For the bulb and its model this change is provided by the coupling between input and feedback gain. Whether in the rest state the bulbar dynamics are governed by a point or a chaotic attractor, the input surge and the attendant increase in gain may cause bifurcation to a limit cycle attractor. Order at high amplitude emerges from low-level chaos, only to collapse again as the gain is reduced with exhalation. In this view the bulbar EEG manifests repeated bifurcations at the rate of respiration, with manifestation of recurrent limit cycle states in the bursts. Each state holds for the entire main bulb for the duration of the bursts on the order of 50–150 ms or more.

3.4. *Odor-specific information in the EEGs.* The information that serves to classify bursts correctly with respect to stimulus condition is uniformly distributed among the amplitude coefficients of the dominant component of the coherent, higher-frequency bursts. This implies that in the presence of a certain odor complex, which most commonly is the

* Mathematicians have pointed out to us that our preliminary estimates³⁵ on the dimensions of the dynamic processes of the bulbar EEG range between 4 and 6, and that these values are inconsistent with the unit dimension of the 'limit cycle' as strictly defined. One proposed alternative, the 'low-dimensional attractor', does not serve to distinguish between our 'orderly' and 'disorderly' events. Another alternative, the 'hyper-dimensional toroid' is unsatisfactory because we have no conception at present of the geometry of our putative attractors in phase space. Moreover, the field of non-linear dynamics has not yet adequately developed its own conventions to handle the description of attractors in spatially distributed systems. Further studies will be needed to devise a more rigorous classification than that we use here.

background or control complex but may be an odorant CS, upon bifurcation the oscillation tends to converge to a definite and reproducible spatial pattern of amplitude modulation. The details of the phase, the center frequency, and the temporal amplitude and frequency modulation are insignificant. The existence of each stable pattern depends on a successful learning process that results in emergence of discriminatory behavior. We infer that for each discriminated odorant a learned limit cycle attractor forms, which is distinguished from others in its class by its basin, mediated by the receptors that were activated during training, and by its spatial amplitude pattern.

A mechanism of synaptic change that we propose to explain these findings is based on earlier studies of the change in the shape of averaged evoked potentials from the prepyriform cortex of cats as they were trained to press a bar for milk in response to electrical stimulation of the lateral olfactory tract^{23,25}. The same coordinated and sustained pattern of change in waveform was found in the bulb on appetitive conditioning of rats to LOT stimulation and in the superior colliculus on appetitive conditioning of cats to optic tract stimulation (unpublished data). The change consisted in a decrease in phase, frequency and decay rate of the dominant damped cosine fitted to the responses.

Simulation of this pattern change with the solutions to piece-wise linear and non-linear differential equations modelling the dynamics of bulb or cortex^{29,35} demonstrates that the only change in the equations that suffices to replicate the change in response waveform is a small increase in the coefficients representing the strength of synapses from excitatory neurons onto other excitatory neurons, that is, by an increase in mutually excitatory feedback gain among elements representing local subsets of excitatory neurons. A modest increase of 40% can increase the sensitivity of a local oscillator 40,000-fold. This is because of the combination of excitatory positive feedback with the amplitude-dependent non-linear gain; small inputs can explode into large outputs providing that they last long enough. The coupling with negative feedback ensures that the output is oscillatory and not monotonic, and that the oscillation terminates after cessation of input.

When the mutually excitatory connections in the model are strengthened among a subset of elements,

for example 8–16 out of an array of 64 oscillators, input to any one or more activates the others preferentially, so that the spatial pattern of output reflects stereotypically the template of the strengthened connections and not the locus of the input. This system closely resembles the nerve cell assembly of Hebb^{52,104}. We conceive that on each inhalation during conditioning an odorant activates multiple receptors within a subclass that is sensitive, and these in turn co-activate a subset of mitral cells. If reinforcement is given, then the bidirectional synapses that couple the concomitantly active neurons are strengthened. Over several trials with 10–20 inhalations on each trial, a large fraction of the subclass of sensitive receptors is stimulated by random selection owing to turbulence in nasal airflow, and the nerve cell assembly is enlarged by pair-wise co-activation of the mitral cells to which they project. Thereafter any input to small numbers of receptors in that fraction activates the entire assembly preferentially.

Recent evidence indicates that reinforcement is mediated in the bulb by norepinephrine presumably under control of the locus coeruleus. Injection of the beta-blocker propranolol into the bulb blocks the EEG pattern changes that otherwise occur on presentation of odorants with shock, whereas intrabulbar infusion of norepinephrine enables pattern changes to odorants without reinforcement, that otherwise do not occur⁴⁷.

In the model and by inference in the bulb, if bifurcation does not occur, the stimulus-evoked activity remains localized to the nerve cell assembly, but with onset of the limit cycle oscillation of the burst, the entire system engages in activity. The stereotypic output pattern is global, both in the sense that it involves all elements and that each local region, such as the fraction of the bulb covered by the array, contains all of the information at reduced resolution compared with the whole. In this respect though not in others bulbar output may resemble a holographic storage pattern.

The significance of the phase extremum for each burst is that it may occur at the site of nucleation, that is, the spatial location at which the bifurcation from chaos to a limit cycle begins. The phase extrema from successive bursts vary at random over the bulbar surface both in location and in sign. The extrema for the dominant and secondary frequency components of

individual bursts tend to conform closely in sign (phase lead or lag) and in location; the conduction velocities, both measured over a part of the bulb flattened by the array, also closely agree. The velocity of apparent propagation, 1.73 m/s, may depend on the conduction velocity of the axon collaterals of mitral cells; the velocity of mitral axon terminal segments in the prepyriform cortex (Fig. 2) is 2 m/s²⁵. From the size of the rabbit bulb (1.5 mm in radius at the depth of the collaterals) and the typical frequency of oscillation (60–70 Hz) the bifurcation is completed in about 1/6 cycle (2.5 ms). The same should hold for the larger bulb of the cat with frequencies of 35–45 Hz¹⁰ and the smaller bulb of the mouse with frequencies of 75–90 Hz²⁰. In these few milliseconds the likelihood of formation of two or more competing sites of nucleation would seem to be small; evidence for it was sought in the form of disparate phase extrema between the dominant and secondary components of orderly and disorderly bursts, but none was found³⁷.

3.5. *The disorderly bursts: chaos?* Close to 20% of

control bursts and 50% of odor bursts of both kinds have broad temporal spectra with multiple peaks, and the largest peak is typically at a frequency between 20 and 40 Hz. The modulation of the center peak frequency commonly exceeds 50% over the recorded duration of the burst (76 ms). The spatial amplitude patterns of the 5 cosine components do not serve to classify bursts and do not fall into reproducible categories. An explanation of these bursts is that they manifest failure of the bulbar mechanism to converge to a limit cycle attractor but possibly to a chaotic attractor.

This type of activity also occurs when rabbits are presented with a novel odor in relatively strong concentration (Fig. 11). Regular bursts of the control state are replaced by low amplitude aperiodic activity having a broad spectrum with its largest peak below 55 Hz. The frequency shift distinguishes it from interburst activity. Our interpretation is that a limit cycle attractor does not exist to serve as a focus for convergence. Almost invariably rabbits orient to the stimu-

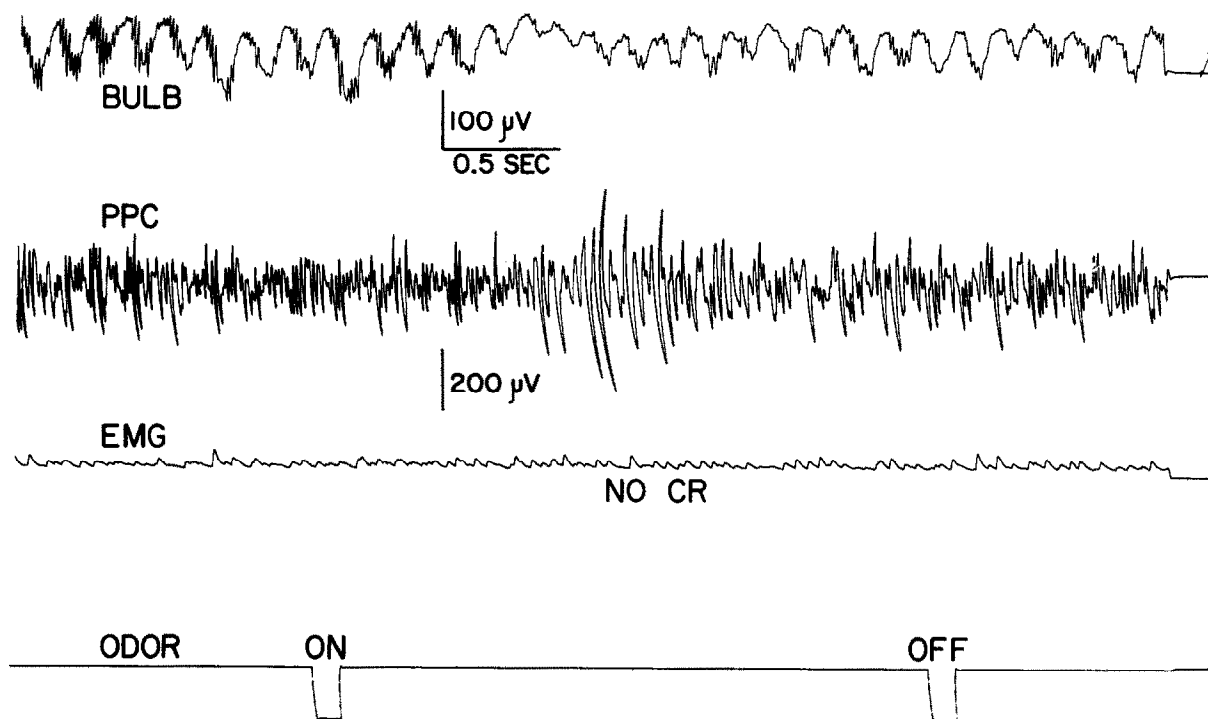


Fig. 11. An example is shown of high-frequency burst suppression in the bulbar EEG by presentation to a rabbit of a novel odorant, which elicited a sniffing response but not a conditioned response (paw flexion) as did an odorant CS⁺. The EEG of the prepyriform cortex (PPC) showed an episode of erratic low frequency activity that we suggest may reflect chaotic as distinct from 'noisy' activity in the bulb and the prepyriform cortex to which it transmits. Evoked potential studies²⁵ suggest that the cortex acts as a resonating receiver with broad response bands in two or more frequency ranges.

lus for several trials; thereafter, both the EEG change and the orienting response abate and disappear, if the odorant is not reinforced. This suggests that the disorderly burst in itself may mediate the orienting response. A possible mechanism is that the prepyriform cortex operates as a tuned filter to which the bulb transmits its oscillatory output. Spectral analysis of the impulse responses reveals multiple resonant peaks, particularly those in the normal transmission range above 55 Hz, but also in the range of 20–40 Hz. Therefore, the disorderly burst may serve first as a signal that convergence to a limit cycle attractor has failed, and thereafter by repetition that an unknown odorant is present, constituting a departure from the status quo. The persistence of the status quo is signalled by the control bursts.

3.6. Limitations of the approach. The first difficulties in spatial analysis were those of hardware in getting enough simultaneous measurements to enable the assembly of spatial images. Thereafter the problems lay in developing the software needed to manage masses of data and extract the significant features. The solutions described here were to use spatial and temporal spectral analysis to determine optimal sampling rates, digital filters to decompose the data into space-time components and residuals, and a behaviorally based assay to evaluate event-related information in the several fractions. The results led to the problem of interpretation; our approach was to embody the known anatomy, physiology and pharmacology of the bulb in a set of differential equations, solve the equations for input, initial and boundary conditions simulating those holding in normal behavior, and compare the solutions of the equations expressed as curves with the results of measurement expressed as data points. When they conformed we transferred our explanation of the dynamics from the model to the bulb, using the languages of neurobiology and non-linear dynamics. The over-riding problem was to maintain the brain in a normal functional state. We solved this by adapting our recording systems for use with permanently placed electrodes in animals subjected to conditioning procedures.

Present problems exist at all levels. One is getting enough sensors on or into the brain for long-enough periods to allow behavioral studies without damaging the brain or impairing the health of the animal. The present limit to 64 channels is imposed more by the

size of the connector cemented to the skull than by the availability of amplifiers, multiplexers, and core to handle the data flow. Another is the restriction to recording from laminar structures, particularly the lissencephalic cortices found in simpler mammals. Management of the difficulties of sampling and 3-D analysis of data from nuclei and folded laminar structures such as the hippocampus seems beyond feasibility at present. So also is the management of data from 64 or more micro-electrodes, although the use of optical sensors seems promising as a source of data on unit activity⁴⁹.

The field potentials such as the EEG suffer from the smoothing effect of the volume conductor especially for scalp electrodes but also for cortical electrodes on and under the surface. In the bulb the attenuation with spatial frequency is 10-fold with each increment of 0.5 c/mm; at the spatial frequency of the glomeruli, which are likely to determine the 'grain' of bulbar macroscopic activity patterns, the attenuation is 10^{-4} , so that the detail of bulbar activity patterns is irretrievably lost from the EEG even with closely spaced electrodes. Surgical access to many parts of the brain is limited either by circulatory vessels, afferent pathways or gyrfication. These shortcomings, are to some extent offset by the robustness of the macroscopic activity. High classification rates of bulbar EEG bursts were found despite restriction of the spatial sample to 1/5 of one bulb, at a spatial sampling frequency 1/4 of the optimal, over a time base 1/10 that available to the animals, and on signals that were often not much above the amplifier and electrode noise levels. In fact the system did slightly better in EEG discrimination than did the animals in responding correctly to odorants^{38,105}.

Limitations also restrict our use of non-linear dynamics to selected simulations of representative events with solutions of the equations by numerical integration. This is less than adequate for constructing representations of the phase space of the model⁷; even could we do this the available algorithms for graphic display might be insufficient. A large part of work being done in non-linear dynamics is devoted to exploring the complex behavior that can be elicited from standard 'simpler systems' such as coupled Van der Pol oscillators; the inverse problem of constructing a model given the behavior cannot be generalized. The bases for model-building in neuro-

physiology are too far removed from those of hydrodynamics, plasma physics, theoretical chemistry, embryology, etc., for more than the exchange of analogs and anecdotes. Diffusion, for example, is replaced by axonal conduction. The dimensions and characteristic exponents of putative EEG limit cycle and chaotic attractors are still under initial study^{6,35}. From the perspective of neurobiologists the bulb is a 'simpler system', but the dynamics of 2000 coupled non-linear oscillators with indefinite numbers of chaotic and limit cycle attractors, continually perturbed by 'noise' and changing state 5–10 times per second, is not so regarded by mathematicians.

Our ability to distinguish chaos from equilibrium under perturbation is inadequate³⁵. The fractal dimensions and Lyapunov exponents have not been measured reliably. Chaos is likely to play major roles, first in the background state as the means for giving rapid access to any of a collection of limit cycle attractors on each inhalation, second as a means for expressing failure of convergence, and third as a vehicle for information of kinds not yet defined. This area of EEG studies will be of major importance in the next decade.

4. IMPLICATIONS FOR NEUROPHYSIOLOGY

4.1. *Sensory systems and perception.* Despite the complexity of its details, spatial analysis offers a simple and compelling answer to the question of how the diverse synaptic input to sensory cortex from multiple and often widely separated axons within the duration of a sniff or a saccadic interval is integrated with past experience into a percept. Our answer is that the input initiates (a) a local spatial pattern of activity that is shaped by a pre-existing nerve cell assembly, and (b) a parametric increase in gain that causes a state change from pre-existing low-level chaos to a high-level limit cycle carrier. The amplitude modulation pattern is selected by the input and shaped by the assembly; each local part of the bulb takes an amplitude of oscillation that is determined by the whole. Each local region transmits the whole with a degree of resolution determined by its size relative to the size of the bulb. Thus the input is local and after the bifurcation the output is global.

The data show that this happens in olfaction; the spatial analysis shows the manner in which it can take

place. The next question is whether this transformation occurs in other sensory systems as well. The likelihood that it does is enhanced by several similarities among sensory systems in structure and function. All contain arrays of receptors that feed in parallel to arrays of neurons, usually through relays but always ultimately to laminated neuropil in cortex. The cortex contains large numbers of densely interconnected excitatory and inhibitory neurons with the requisite 3 kinds of synaptic feedback. Again the output of cortex is in parallel by large numbers of axons. Although the bulb has many specialized anatomical and physiological traits peculiar to it, the only properties needed for the simulation of its key operations are those that it has in common with other systems: parallel input and output and synaptically coupled masses of excitatory and inhibitory neurons with the voltage-dependent membrane conductance of the action potential.

In our view sensory processing is in two stages: analysis and synthesis. Receptors transduce incident energies at points on the array surface with varying degrees of specificity to the various qualities of the stimuli. Their axons convert generator potentials to pulse trains and transmit them into the central nervous system with a mix of convergence and divergence. The receptor fields of second and third order neurons provide evidence that receptors establish local fields of activity, and that interactions among the target neurons and interneurons perform several analytic operations, among them the taking of local spatial and temporal derivatives (revealed by 'edge' and 'moving spot' detectors), dynamic range compression, normalization, clipping and holding. Evidence has been found that each of these operations in the olfactory bulb is performed by the various types of periglomerular cells in the outer layers of the bulb. Although they are less sophisticated than the analogous operations especially in the visual and somesthetic systems, the end result is the same: a particular stimulus establishes a particular collocation of neural activity within a cortical projection zone, or more likely a set of collocations in an array of cortical parcels that reflect the outcomes of different kinds of local analysis.

Synthesis in the bulb is through bifurcation from the chaotic state of sensory input to the oscillatory state of output to the olfactory cortex. Herein is a salient difference between the olfactory and other sen-

sory systems, because the high-amplitude bursts of oscillation that characterize the olfactory EEG are not seen elsewhere in the brain. EEG activity of neocortex in the beta range (15–35 Hz) is relatively muted, and almost nothing is known about neocortical activity in the gamma range (35–90 Hz) other than the fact that it exists in many parts of neocortex of healthy adults^{71,95}. In our view this EEG difference stems from differences in cytoarchitecture and not from differences in neural interconnections. The 3 brain structures with the most obvious gamma components in their EEGs are the bulb, the prepyriform cortex and the hippocampus. All 3 have strikingly well developed lamination of their neurons. By way of contrast the cerebellum has equally striking lamination but no significant oscillations in the range from 1 to 100 Hz; however, its main neural inhibitory connections form feed-forward and not feedback loops. The neurons in neocortex are vertically dispersed, and they are segregated into layers at greater depths. These features enhance the smoothing effect of the volume conductor, especially for summed dendritic potentials at higher temporal frequencies, so that EEG activity in the theta (3–7 Hz) and alpha ranges (8–14 Hz) is relatively far more prominent in neocortex than in paleocortex. Of course the spectral smoothing is still stronger for scalp recordings^{43,86}.

Analysis of field potentials and synthesis of explanatory models are arduous and time-consuming. Some of the many steps have been touched on in this essay. Spatial analysis may offer a short-cut to answer the key question in neocortex, whether bifurcation from low-level chaos to a limit cycle or chaotic attractor integrates sensory input into a pattern corresponding to a percept. The test would involve placing arrays of electrodes at appropriate intervals determined from the spatial spectrum onto the surface of a sensory cortex, the superior colliculus, or CA1 of the hippocampus, in order to test whether the spatial amplitude patterns of beta and/or gamma activity (not necessarily periodic) fall into distinct clusters, depending on the presence of two or more stimuli to which a subject has been trained to respond differentially. The techniques of spatial bandpass filtering and deconvolution can be combined empirically to sort out activity patterns in dipole layers stacked vertically below the cortical surface as in the olfactory bulb^{31,35,76}. A degree of success in this direction has already been

achieved through scalp-recording of event-related potentials (ERPs) in humans^{43,62}, but the results are merely statistical, depend too strongly on ensemble time-averaging, and are from too few channels. If the time-dependence of sequential episodes of spatial coherence were to be determined from spatial analysis, a basis might emerge for re-investigation of the neural mechanisms of thalamocortical gating^{4,101}, as the basis for the sequencing of perceptions²².

4.2. Implications for motor systems and pattern generators. The neural mechanisms of motor activity are ripe for description with non-linear dynamics, especially rhythmic processes in respiration¹³, locomotion⁴⁸, bird song¹⁰⁸ and speech⁶³. The terms 'attractor' and 'pattern generator' are not quite synonymous, the one referring to a property of a neural mass, that it enters and sustains an identifiable pattern of activity, and the other to the expression of that property in an identifiable pattern of muscular activity. An attractor can explain or account for a pattern generator. Owing to limitations already discussed, the use of spatial analysis may be limited in the near future, except for studies of the motor cortex.

Use of the concept of an attractor is predicated on some knowledge of a collection of attractors, the changes in system parameters that support bifurcation from one to another, the basins of input for each, and the separatrices that demarcate boundaries of the basins, together comprising the phase portrait of the system under study¹. The analysis of sensory systems is made feasible by control of the input; the comparable development for motor systems may require tracing the outputs from sensory systems. Essentially this is the problem of sensori-motor integration. While it is complex, we suggest that it is not remote, and that we must prepare to deal with it immediately on investigating further processing of the outputs of the bulb and sensory cortex.

The problem comes directly to the fore in the form of odorant concentration. One of the key unsolved problems in olfaction is unravelling the mechanisms by which information about odorant concentration is processed. In other sensory and motor systems the quality of a stimulus or motor command is thought to be conveyed in the selection of active neurons and their spatial location, while the intensity is conveyed in unit firing rates and by recruitment in a pool of similar neurons. In olfaction the individual receptors and

mitral cells appear in amphibia^{18,55,61} and mammals^{15,75,77} to have relatively narrow concentration ranges compared with the ranges of psychophysical identification¹². Despite difficulties from adaptation and response variability⁹⁰ the intensity function has been found to resemble an inverted 'U' rather than a sawtooth^{18,60,75}. Verification of recruitment is problematic owing to the difficulty of recording multiple single units, the immense numbers of receptors, and the confounding variables of rate and direction of air flow over the complexly folded turbinate bones, adaptation, attentional and motivational factors, etc. The amplitude of EEG bursts is clearly not directly related to concentration, nor is the amplitude of the respiratory wave. In psychophysics the absolute identification of odorant concentration is limited to a few steps, for example, strong, moderate, or faint. It is not uncommon for a subjective qualitative change to be reported by humans at a step along a concentration gradient. This suggests that two or more learned limit cycle attractors might form over the basins of receptors active within successive concentration ranges, and that the generalization across these into a larger class might depend on the formation of a higher-order attractor either in the bulb or among the target systems of the bulb.

The detection of relative concentration might seem simpler than the specification of absolute values, but in fact it is more complex, because it requires temporary retention of the results from sequences of inhalations. In normal behavior this sensory information must immediately be integrated with motor information. Relative concentration is determined by repetitive sniffing with exploratory movements of the head and body. A dog, for example, may leap into the air and waggle its nose transversely to its direction of locomotion. The classic search pattern for animals as diverse as dogs, fish and butterflies is movement along lines at right angles to the flow of air or water carrying an odorant plume, with periodic 180° turns upstream at the edges of the plume. Where and how these kinds of information are carried and combined are unknown.

A useful premiss from which to tackle this problem might be to treat the bulb as sensory cortex and the prepyriform and periamygdaloid as motor cortex, analogous to the neocortical sensori-motor cortex. Measurement of the prepyriform averaged evoked

potential has shown that the covariance of the parameters from the cortical waveform accounts for 20% of the variance in the rate of work by hungry cats for food²⁴. The rms amplitude of prepyriform EEGs is also closely related to the rate of work for food²⁵. Bilateral removal of the olfactory bulbs results in secondary degeneration in the prepyriform cortex⁸ and in disordered behavior that parallels severe depression in humans⁵⁶. The same syndrome follows bilateral lesions of 60–80% of prepyriform cortex in cats; complete destruction results in death (unpublished data). Severe depression is known to accompany bilateral basal tuberculous meningitis in humans. When excessively intense electrical stimuli are given to the lateral olfactory tract, the prepyriform cortex enters into a petit mal-like seizure with EEG spikes regularly repeating at 3–4/s. The animals display *absence* (failure to respond to stimuli but without loss of consciousness) and repetitive twitches of the face and jaw synchronously with the spikes²⁵. These are also the rates at which sniffing, chewing, licking and lapping occur, together with synchronized EEG fluctuations that may in larger part be due to concomitant variations in nasal air flow. Perhaps the seizure locks onto a characteristic frequency in the cortical mechanism underlying these facial and jaw movements. They are lost following paleodecortication. This may be analogous to the loss of placing, hopping and grasping reflexes after lesions to sensori-motor neocortex, because all of these movements involve orientation of parts of the body to objects or events in the world outside of the body.

The distinction between bursts and burst sequences corresponds to that between 'pop-out' or 'pre-attentive' and 'attentive' visual processing⁵⁹, and between 'parallel' and 'serial' processing in AI systems generally. Our emphasis as experimentalists on knowing what the animal is doing during the time frame of stimulus presentation stems from our belief that, in any time frame much exceeding 0.1 s, proprioceptive and reafferent information is thoroughly mixed with sensory information in the brain. We expect that attempts to locate process-specific information in spatial patterns of neural activity by classification and correlation will be unsuccessful unless both stimulus and response are measured with behavioral techniques. This is obvious already in the necessity for measurement of respiration and the successful

use of conditioning in order to measure odor-specific information in the bulb at the first synaptic relay. Even this is inadequate here and at more central stations; we must also specify the purposive context in which the recordings are made. We do this now implicitly in terms of 'aversive' and 'appetitive' conditioning used to establish an appropriate type of 'motivation', but we need more explicit contextual detail.

4.3. *Goal-directed behavior.* Sensorimotor integration occurs in the context of goal-directed behaviors such as search, attack and evasion, that are characterized by flexibility in contrast to the relatively stereotypic movements in reflex and robotic behavior. Every movement changes the sensory input, and the new stimulus conditions modify the motor output. The directedness may become apparent to an observer only after the completion of some perseverative sequence of interactions by an animal with its environment, including modification of its surroundings. Commonly it is postulated that the animal brain may generate a central image or representation of a future state of activity or of sensory input, and that action is initiated and sustained until the present state conforms by matching to a centrally maintained image of the projected future state³². By extrapolation from our new findings we believe that purpose does not emerge in the form of a representation of a future state. Instead, we conceive it as the existence of a hierarchy of attractors in the dynamics of large masses of neurons, such that the behavior of the central nervous system and therefore the animal evolves from the present state with a tendency to arrive at a definite future state. No representation is involved; metaphorically we can claim that animals 'predict' future states, but in the absence of a capability for language the word 'foretell' in a strict sense is meaningless.

The remote origin of purposive behavior is in the embryology of the brain, wherein form and function interact to generate a predictable sequence of changes leading from the fertilized ovum to the newborn. No one believes any longer that the form of the infant is expressed at any stage of the embryo as a template to which growth must conform; the goal is implicit. The same self-organizing processes continue after birth, but with an enormous increase in the interactive exchange between the brain and the environment, compared with the sheltered conditions

of the womb or the shell. Just as embryonal development can be described by a trajectory through a sequence of stages, each expressing an attractor that prepares the way for the next, so also can purposive behavior such as search-attack-ingest-digest, but with the difference that the trajectory both within and between stages is crucially and not adventitiously influenced by the environment. The brain both ingests and transforms those aspects of the world that are accessible to it.

The task for spatial analysis is to construct a theoretical framework in which the dynamics of purposive behavior can be incorporated for experimental testing. Two considerations may simplify this task. One concerns the time frame; the essential or archetypal events can take place within one or two seconds required for search and approach by animals trained to find food. This time span comprises the psychological 'here-and-now' in which sequences of sensory and motor events are fused in the context of a trajectory encompassing the goal. The other concerns the brain locus of this on-going synthesis. We have known for a century from the demonstration by Goltz on decorticate dogs that the paleocortex is sufficient to sustain goal-directed behavior; high decerebration shows that it is necessary. In primitive vertebrates such as the tiger salamander⁵⁴ the forebrain that generates purposive behavior consists solely of the prologs of the paleo- and archicortical portions of the limbic system³². The bulb together with a dorsal transitional zone receiving thalamic afferents comprises the anterior sensory third of each hemisphere. The prepyriform cortex and amygdalo-striatal complex constitute the lateral and motor third. The septo-hippocampal formation forms the medial third; recent physiological and behavioral⁸⁷ evidence indicates that this is the locus of the 'cognitive map' inferred by Tolman¹⁰³ to exist in the brain, that might serve as the space-time matrix or 'short-term memory' in which sequential information is assembled.

Purpose might best be conceived, in mathematical terms, as a trajectory of directed movement in phase space through an ordered sequence of basins and bifurcations. In behavior, such a trajectory is expressed by a sequence of purposive actions leading to a goal. The description of such a trajectory requires a higher level of complexity than can be achieved by consideration only of the dynamics of the bulb. We

propose that a mathematical or conceptual approach be undertaken by describing the dynamics of the several parts of the limbic system in much the same terms as for the bulb, and by assembling these in their proper interactive modes. There are few data available as yet on the spatial properties and non-linear dynamics of these other structures^{68,74}, but a speculative overview might help in the collection of new data. We should include in this view the structures identified above as well as others closely affiliated, such as the anterior olfactory nucleus and tubercle and the entorhinal cortex. All contain interconnected populations of excitatory and inhibitory neurons indicating that they maintain the 3 types of feedback relations found in the bulb. The olfactory cortex and hippocampus are still more closely similar to the bulb in having the three-layered architecture that is characteristic of paleocortex. The olfactory nucleus, cortex, amygdaloid, septum and hippocampus all generate EEG activity with prominent components in the range characteristic of bulbar carrier waves, the gamma activity, and also a prominent low frequency component, the theta activity, that may coincide⁷⁴ with the respiratory frequency of rabbits in sniffing (3–7 Hz), and that we view as a gating frequency for bursts of the carrier. Models of the dynamics of the olfactory cortex and of the hippocampus very similar to that of the bulb have been successful in simulating their evoked potentials and impulse firing patterns^{25,68}.

We have devised a logical scheme for describing the interactions of these neural masses in terms of an open-ended hierarchy of K sets²⁵. At the base is a K0 set of elements representing a collection of single neurons that have a common source of input, a common sign of output (either excitatory or inhibitory), but no interaction among them. A KI set represents a mass of neurons having common input and sign of action (either KI_e or KI_i) and also locally dense interactions of each neuron with many others in its surround giving positive feedback. A KII set combining KI_e and KI_i sets represents the negative feedback interaction between excitatory and inhibitory neural masses. Whereas KI sets are capable of slowly changing or sustained activity with different kinds of spatial patterning (stereotypy for the KI_e, spatial contrast for the KI_i), oscillation in the gamma range first appears at the KII level.

We propose that the dynamics of each of the parts

of the limbic system can be described by the same integrodifferential equations that simulate KII bulbar dynamics, along with KI sets that are required to describe subsidiary interneuronal masses, such as the periglomerular neurons in the bulb, the deep pyramidal neurons in the olfactory cortex, and the dentate fascia in the hippocampus. Each of these structures has reciprocal (feedback) connections with contiguous or nearby structures. We suggest that the interactive masses which form the major part of the limbic system and are modelled by KI and KII sets should be represented by a KIII set. Examples include the olfactory bulb, nucleus and cortex; the corticomedial and lateral amygdaloid nuclei and the olfactory striatum; and the septum, hippocampus and subiculum. Beyond this step is the interconnection of the sets for these parts into a dynamic whole to represent the limbic system by a KIV set.

The vertical segregation into a hierarchy is necessary for several reasons. First, each of the parts in itself is sufficiently complex to warrant detailed exploration of its dynamics and its relevant stable states. Second, the description of an orderly sequence of transitions between stable states, such as the trajectory of purpose, will require the collapse of the details of each of the parts into a small number of variables and parameters, so that a state variable at a higher level may serve as a control parameter at a lower level. Third, the anatomical structures and patterns of interconnection and interaction of the limbic system indicate that successive levels of integration and organization of different kinds take place in the formation and operation of the limbic system. For example, the operations of long projection pathways such as the fornix and the olfactory tracts cannot be incorporated into KII sets owing to their attendant delays, temporal dispersions and spatial divergences. Finally, to the extent that we require a hierarchy of meaning to understand different kinds of behavior, we will require a hierarchy of functional states to explain them.

4.4 *A retraction on 'representation'*. Commonly it is said that a stimulus is encoded in or stored as or represented by a pattern of activity, as though a certain token or symbol or message were introduced into the brain along with a certain meaning⁹⁷. Likewise it is postulated³² that in toto the brain sustains a world view, image, model or representation of the

environment, that is continually updated by new input, and that provides the basis for patterned output or action. Thus recognition is conceived as based on comparison of a stimulus-evoked activity pattern with each of a store of pre-existing patterns, and decision as the selection from a store of motor patterns of one that is optimal according to certain rules that are also encoded and exercised perhaps in the manner of a binary decision tree. Actions can result from representations serving centrally in the manner that stimuli do peripherally.

The results from spatial analysis of the olfactory EEG fail to support this interpretation in respect to odors. At one stage of the investigation it seemed that an EEG spatial pattern established during conditioning with an odorant persisted in the absence of the odorant, and we inferred that this pattern might manifest a 'search image'³⁵ for the expected odor³³. However, the present results showed that the data on which this interpretation was based were inadequate for two reasons. Conditioning was serial to one odorant at a time rather than discriminative between two odorants, and the resolution of spatial patterns of EEG amplitude was inadequate. An essential corollary was disproven; if the quality of an expected odor were to take the form of an amplitude pattern, then the presence or absence of that odor would be signalled by the phase pattern³⁰. This was found not to be the case³⁷. Moreover, this interpretation failed to handle effectively the problems of how animals can expect more than one odor at the same time, or respond to novel or unexpected odors, nor did it effectively deal with the fact that bursts occur continually in the control state with the background odor complex.

In the light of present evidence it might be proposed that a search image exists in the form of a limit cycle attractor with its attendant basin of receptor-mediated input, and that multiple search images co-exist as attractors in the bulb to represent those odors that the animal has learned to identify. There are several difficulties with this interpretation. First, it is unnecessary. The concept of an attractor simply constitutes a prediction that given a specified initial condition, the bulb and the animal will tend to behave in a certain way. The behavioral and electrophysiological data speak for themselves without reference to 'representation'. Second, it is inconsistent. A 'ten-

dency' cannot 'represent' anything. In the bulb a tendency is let loose by a stimulus, but the end result of the tendency in a burst pattern cannot play a role in its selection by the stimulus, because the pattern exists after the stimulus and not before. Yet representation by a 'search image' requires that some pattern pre-exist the stimulus. If that pattern were ascribed to one of a collection of synaptic 'templates' created in the bulb by learning, then odor identification would require a systematic search through the collection. If the odor is novel, the entire collection must be reviewed. But animals respond to novel odors in short time spans that are inconsistent with the time required for an exhaustive review of all the odors that we suppose adult rabbits have learned to identify, as indeed they must in order to survive in an ever-changing environment. Hence neither an EEG pattern, nor an attractor, nor a synaptic template is consistent with the physiological properties predicated for a representation as a stored, retrievable information pattern that serves to classify stimuli.

Other difficulties must be dealt with concerning classifications, associations, meanings and other aspects of representations, exemplified by the difficulties of stating exactly what is being represented, at which time, by which part to which other part of the brain. The root of these difficulties is that the referents, contexts and meanings of representations are invariably in the brain of the observer and not that of the observed. If, as we propose, each brain is self-organizing with its own frames of reference, then mapping from one to another is problematic. However, it should suffice in neurophysiology that the concept is inconsistent with the data and unnecessary. The same reasoning holds a fortiori for more specific formulations such as codes, images, signals, files, tables, plans, rules, models, schemata, lists, clocks, programs, scripts, frames, symbols, etc. Thus, in the language of representation the olfactory bulb extracts features, encodes odor information in patterns of neural activity, recognizes odor stimulus patterns, identifies odor figures in olfactory grounds, represents expected odors, forms olfactory search images, tests hypotheses on learned olfactory expectations, and stores and retrieves olfactory engrams. These and other seductive phrases seem to say something, but in animal physiology they are empty rhetoric that leads nowhere. They are not merely wrong; they are irrele-

vant and misleading. It is our conclusion that animals interact with their environments but need not and do not represent them in doing so. An ultimate goal in neurophysiology is to explain human consciousness and our capacity for representation, but experiments on animal brains will not directly support that, and the concept should not be part of its explanation.

5. SUMMARY

Spatial analysis with preamplifier arrays and computers offers fresh perspectives on brain function. Realization of its potential depends on development of appropriate procedures for data processing and display, experimental paradigms to serve as benchmarks, and theories of brain function to predict what to look for and how to distinguish valid results from artifacts. Measurement of EEGs from arrays of 64 electrodes chronically implanted on the olfactory bulbs of rabbits that are trained to discriminate odorant conditioned stimuli show that the odorants induce spatially distinctive amplitude patterns of neural activity. The odor-specific information density is inferred to be uniform over the whole main bulb. The neural dynamics that produce these activity patterns emerge from the synaptically interactive sheet of excitatory mitral and inhibitory granule cells with distributed input and output tracts and with static non-

linearities deriving from the nerve impulse mechanism. Excitatory synapses between mitral cells are subject to modification when odorants are paired with unconditioned stimuli, thus forming nerve cell assemblies. Odorant-specific information established by a stimulus locally in the bulbar unit activity is integrated with past experience by an assembly, disseminated over the entire bulb on the order of 100 mm² in area in a time period of 2.5 ms, and sustained for a time period on the order of 0.1 s. An arbitrary spatial sample on the order of 20% of bulbar EEG activity captures the entire integrated information albeit at lesser resolution than the whole. This synaptic mechanism of local input and global output may be common to all of the cerebral cortex. The implications are discussed for neocortical sensory systems, motor pattern generators, and goal-directed behavior in the context of self-organizing non-linear dynamic systems.

ACKNOWLEDGEMENTS

Supported by Grants MH06686 from the National Institute of Mental Health and NS16559 from the National Institutes of Health. Discussions with Bill Baird, Frank Eeckman, Kamil Grajski and Michael Shadlen are gratefully acknowledged.

GLOSSARY

Structural terms

neural mass: a large collection of neurons of the same or differing types, generally contiguous and with intertwined filaments²⁵.

K-set: the mathematical representation of a mass, defined hierarchically in terms of commonality of input and type(s) of internal interaction²⁵.

nerve cell assembly: a subgroup within a mass of excitatory neurons that are linked by synapses strengthened during learning^{52,104}.

neural template: the spatial structure formed by a nerve cell assembly³².

Functional terms

neural activity (microscopic): the sequence of action potentials of neurons one at a time, or the

magnitude of membrane depolarization at a trigger zone.

neural activity (macroscopic): the magnitudes of dendritic currents or of axonal potentials locally averaged among neurons of like kind in a mass and occurring at all points and times over the mass for an extended time interval.

activity density function: the abstract conception of neural activity over a K-set as pulse densities (axonal) and wave densities (dendritic)²⁵; equivalent to Sherrington's⁹⁶ central excitatory state (c.e.s.).

state variable: the mathematical representation by a symbol of a pulse or wave density function in a K-set.

observable: a sequence of single or multiple unit potentials or of field potentials recorded mo-

nopolarly, that manifests neural activity, and that with appropriate transformations is used to evaluate a state variable by curve-fitting.

burst: an observable; a brief, high-frequency fluctuation observed in field potential whether or not it is periodic, which rises in amplitude above the background level and then disappears.

wave packet: a type of macroscopic pulse and wave activity that is manifested by a burst; it is inferred to occupy a delimited volume of tissue (hence, package or packet), to have certain characteristic temporal and spatial frequencies (hence, wave), and to involve expenditure of neural metabolic energy above the background level³².

operation: a mathematical description of the transformation effected by an operator; in linear analysis it is defined by the ratio of input to output; in non-linear analyses involving structural or parametric changes the definition is less general and more complex.

operator: an agency imposing a change from one state of activity to another; a wave packet is conceived as an operator, because it changes the activity of a neural mass into which it is transmitted by axons³².

attractor: the property of a dynamic system that is manifested by the tendency under various but delimited conditions to go to a reproducible active state and stay there; the wave packet is the

actualization of an attractor, and the burst is its observable manifestation.

trajectory: a mathematical description of the sequence of values taken by a state variable in going from an initial or starting condition to an attractor, or through a sequence of attractors¹.

Behavioral terms

pattern generator: a mass of neurons whose dynamics is dominated by one or more attractors, and whose activity is correlated with patterns of motor activity identified by an observer, e.g. respiration, locomotion, song.

search image: the selective, learned sensitivity of an animal to a particular stimulus identified by an observer, that is predicated on an attractor in the dynamics of a neural sensory system^{5,33}.

purpose: the quality of directedness in behavior that is discerned or manipulated by an observer, and that is predicated on the existence of multiple attractors and a trajectory through them.

representation: a general term used to denote correspondence between a stimulus or response and a hypothetical brain state, that might be sought by correlation between the reproducible space-time pattern of an observable and a repeated stimulus or response defined by the observer; the concepts of storage, read-out and other manipulation of a representation have been defined for computer systems but not for neural systems.

REFERENCES

- 1 Abraham, R.H. and Shaw, C.D., *Dynamics, The Geometry of Behavior*, Ariel Press, Santa Cruz, CA, 1983, 220 pp. (part 1), 137 pp. (part 2), 1985, 121 pp. (part 3).
- 2 Adrian, E.D., The electrical activity of the mammalian olfactory bulb, *Electroencephalogr. Clin. Neurophysiol.*, 2 (1950) 377-388.
- 3 Amoore, J.E., Olfactory genetics and anosmia, *Handbook of Sensory Physiology*, 4 (1971) 245-256.
- 4 Andersen, P. and Andersson, S.A., *Physiological Basis of the Alpha Rhythm*, New York, Appleton-Century-Crofts, 1968, 235 pp.
- 5 Atema, J., Holland, K. and Ikehara, W.F., Olfactory responses of yellowfin tuna (*Thunnus albacares*) to prey odors, *J. Chem. Ecology*, 6 (1980) 457-465.
- 6 Babloyantz, A. and Nicolis, C., Reconstruction of the dynamics of the electrical activity of the brain. In prep.
- 7 Baird, B., Nonlinear dynamics of pattern formation and pattern recognition in rabbit olfactory bulb, *Proc. Conf. Evaluation, Games and Learning*, Los Alamos 20-24 May 1985, Physica D, in press.
- 8 Becker, C.J. and Freeman, W.J., Prepyriform electrical activity after loss of peripheral or central input or both, *Physiology and Behavior*, 3 (1968) 597-599.
- 9 Bressler, S.L., Spatial organization of EEGs from olfactory bulb and cortex, *Electroencephalogr. Clin. Neurophysiol.*, 57 (1984) 270-276.
- 10 Bressler, S.L. and Freeman, W.J., Frequency analysis of olfactory system EEG in cat, rabbit and rat, *Electroencephalogr. Clin. Neurophysiol.*, 50 (1980) 19-24.
- 11 Buchsbaum, M.S., Rigal, F., Coppola, R., Cappelletti, J., King, C. and Johnson, J., A new system for gray-level surface distribution maps of electrical activity, *Electroencephalogr. Clin. Neurophysiol.*, 53 (1982) 237-242.
- 12 Cain, W.S. and Engen, T., Olfactory adaptation and the scaling of olfactory intensity. In C. Pfaffman (Ed.), *Olfaction and Taste III*, Rockefeller Univ. Press, New York, 1969, pp. 127-141.
- 13 Cohen, M., Neurogenesis of respiratory rhythm in the mammal, *Physiol. Rev.*, 59 (1979) 1105-1173.
- 14 Coopersmith, R. and Leon, M., Enhanced neural re-

- sponse to familiar olfactory cues, *Science*, 225 (1984) 849–851.
- 15 Daval, G. and Levetau, J., Réponses unitaires des cellules mitrales du bulbes olfactifs de lapin à une stimulation odorante d'intensité variable, *C.R. Acad. Sci. Paris*, 295 (1982) 637–640.
 - 16 Davis, G.W. and Freeman, W.J., On-line detection of respiratory events applied to behavioral conditioning in rabbits, *IEEE Trans. Biomed. Engineering*, 29 (1982) 453–456.
 - 17 Døving, K.B. and Pinching, A.J., Selective degeneration of neurones in the olfactory bulb following prolonged odor exposure, *Brain Res.*, 52 (1973) 115–129.
 - 18 Duchamp, A., Electrophysiological responses of olfactory bulb neurons to odour stimuli in the frog. A comparison with receptors cells, *Chem. Senses*, 7 (1982) 191–210.
 - 19 Eastman, C., Construction of miniature electrode arrays for recording cortical surface potentials, *J. Electrophysiol. Tech.*, 5 (1975) 28–50.
 - 20 Eckert, M. and Schmidt, U., The influence of permanent odor stimuli on the postnatal development of neural activity in the olfactory bulbs of laboratory mice, *Dev. Brain Res.*, 20 (1985) 185–190.
 - 21 Edelman, G.M. and Mountcastle, V.M., *The Mindful Brain*, MIT Press, Cambridge, MA, 1978, 100 pp.
 - 22 Efron, R., The minimum duration of a perception, *Neuropsychologia*, 8 (1970) 57–63.
 - 23 Emery, J.D. and Freeman, W.J., Pattern analysis of cortical evoked potential parameters during attention changes, *Physiol. Behav.*, 4 (1975) 69–77.
 - 24 Freeman, W.J., Correlation of goal-directed work with sensory cortical excitability, *Recent Adv. Biol. Psychiatry*, 7 (1964) 243–250.
 - 25 Freeman, W.J., *Mass Action in the Nervous System*, Academic Press, New York, 1975, 489 pp.
 - 26 Freeman, W.J., Spatial frequency analysis of an EEG event in the olfactory bulb. In D.A. Otto (Ed.), *Multidisciplinary Perspectives in Event-Related Brain Potential Research*, U.S. Government Printing Office, Washington, EPA-600/9-77-043, (1978) 531–546.
 - 27 Freeman, W.J., Spatial properties of an EEG event in the olfactory bulb and cortex, *Electroencephalogr. Clin. Neurophysiol.*, 44 (1978) 586–605.
 - 28 Freeman, W.J., Nonlinear gain mediating cortical stimulus-response relations, *Biol. Cybernet.*, 33 (1979) 237–247.
 - 29 Freeman, W.J., Nonlinear dynamics of paleocortex manifested in the olfactory EEG, *Biol. Cybernet.*, 35 (1979) 21–34.
 - 30 Freeman, W.J., EEG analysis gives model of neuronal template-matching mechanism for sensory search with olfactory bulb, *Biol. Cybernet.*, 35 (1979) 221–234.
 - 31 Freeman, W.J., Use of spatial deconvolution to compensate for distortion of EEG by volume conduction, *IEEE Trans. Biomed. Engineering*, 27 (1980) 421–429.
 - 32 Freeman, W.J., A physiological hypothesis of perception, *Perspectives in Biology and Medicine*, 24 (1981) 561–592.
 - 33 Freeman, W.J., The physiological basis of mental images, *Academic Address, Biol. Psychiatry*, 18 (1983) 1107–1125.
 - 34 Freeman, W.J., Dynamics of image formation by nerve cell assemblies. In E. Basar, H. Flohr and A.J. Mandell (Eds.), *Synergetics of the Brain*, Springer-Verlag, Berlin, 1983.
 - 35 Freeman, W.J., Techniques used in the search for the physiological basis of the EEG. In A. Gevins and A. Remond (Eds.), *Handbook of Electroencephalography and Clinical Neurophysiology*, Elsevier, Amsterdam, 1985, Vol. 3A, Part 2, Ch. 14, in press.
 - 36 Freeman, W.J., Correlation of olfactory EEG with behavior: Time series analysis, submitted.
 - 37 Freeman, W.J. and Baird, B., Correlation of olfactory EEG with behavior: spatial analysis, submitted.
 - 38 Freeman, W.J. and Grajski, K.A., Correlation of olfactory EEG with behavior: factor analysis, submitted.
 - 39 Freeman, W.J. and Schneider, W.S., Changes in spatial patterns of rabbit olfactory EEG with conditioning to odors, *Psychophysiology*, 19 (1982) 44–56.
 - 40 Freeman, W.J. and Viana Di Prisco, G., EEG spatial pattern differences with discriminated odors manifest chaotic and limit cycle attractors in olfactory bulb of rabbits, *Proceedings, Conference on Brain Theory*, Trieste. Berlin, Springer-Verlag, 1985, in press.
 - 41 Freeman, W.J., Viana Di Prisco, G., Davis, G.W. and Whitney, T.M., Conditioning of relative frequency of sniffing by rabbits to odors, *J. Comp. Psychol.*, 97 (1983) 12–23.
 - 42 Garfinkel, A., A mathematics for physiology, *Am. J. Physiol.*, 245 (1983), (*Regul. Integr. Comp. Physiol.*, 14, R455–R466).
 - 43 Gevins, A. and Remond, A. (Eds.), *Handbook of Electroencephalography and Clinical Neurophysiology*, Elsevier, Amsterdam, 1985, Vol. 3A, Part 2: Analysis of Brain Electrical and Magnetic Signals, in press.
 - 44 Gonzales, R.C. and Wintz, P., *Digital Image Processing*, Addison-Wesley, Reading, MA, 1977, 431 pp.
 - 45 Gonzalez-Estrada, M.T. and Freeman, W.J., Effects of carnosine on olfactory bulb EEG, evoked potentials and D.C. potentials, *Brain Res.*, 202 (1980) 373–386.
 - 46 Grajski, K.A., Breiman, L. and Freeman, W.J., Tree-structured methods classify spatial patterns of bulbar EEG amplitude, *Neurosci. Abstr.*, 10 (1984) 331.17, p. 1143.
 - 47 Gray, C.M., Freeman, W.J. and Skinner, J.E., Associative changes in the spatial amplitude patterns of rabbit olfactory EEG are norepinephrine dependent, *Neurosci. Abstr.*, 10 (1984) 36.2, p. 121.
 - 48 Grillner, S., Neurobiological bases of rhythmic motor acts in vertebrates, *Science*, 228 (1985) 143–149.
 - 49 Grinvald, A., Manker, A. and Segal, M., Visualization of the spread of electrical activity in rat hippocampal slices by voltage-sensitive optical probes, *J. Physiol. (London)*, 333 (1982) 269–292.
 - 50 Haberly, L.B., Unitary analysis of opossum prepyriform cortex, *J. Neurophysiol.*, 36 (1973) 762–774.
 - 51 Hassler, A.D. and Scholz, A.T., *Olfactory Imprinting and Homing in Salmon*, Springer-Verlag, New York, 1983, 134 pp.
 - 52 Hebb, D.O., *The Organization of Behavior*, Wiley, New York, 1949, 333 pp.
 - 53 Helleman, R.H.G. (Ed.), *Nonlinear Dynamics*, N.Y. Acad. Sci., New York, 1980, 507 pp.
 - 54 Herrick, C.J., *The Brain of the Tiger Salamander*, Univ. Chicago Press, Chicago, IL, 1948, 407 pp.
 - 55 Holley, A., Duchamp, A., Revial, M.F., Juge, A. and MacLeod, P., Qualitative and quantitative discrimination in the frog olfactory receptors: analysis from electrophysiological data, *Ann. N.Y. Acad. Sci.*, 237 (1974) 102–114.
 - 56 Jesberger, J.A. and Richardson, J.S., Animal models of

- depression: parallels and correlates to severe depression in humans, *Biol. Psychiatr.*, 20 (1985) 764–784.
- 57 John, E.R., Switchboard versus statistical theories of learning and memory, *Science*, 177 (1972) 850–864.
- 58 Jourdan, F., Spatial dimension in olfactory coding: a representation of the 2-deoxyglucose patterns of glomerular labeling in the olfactory bulb, *Brain Res.*, 240 (1982) 341–344.
- 59 Julesz, B., A brief outline in the texton theory of human vision, *Trends in Neurosci.*, 7 (1984) 41–45.
- 60 Kauer, J., Response patterns of amphibian olfactory bulb neurones to odor stimulation, *J. Physiol. (London)*, 243 (1974) 695–715.
- 61 Kauer, J. and Shepherd, G.M., Mechanisms for processing of odour concentration in salamander olfactory bulb neurones, *J. Physiol. (London)*, 252 (1975) 49–50.
- 62 Karrer, R., Cohen, J. and Tueting, P. (Eds.), Brain and Information: Event-Related Potentials, *Ann. N.Y. Acad. Sci.*, 425 (1984) 768 pp.
- 63 Kelso, J.A.S. and Tuller B., 'Compensatory articulation' under conditions of reduced afferent information. A dynamic formulation, *J. Speech Hear. Res.*, 26 (1983) 217–224.
- 64 Laing, D.G., Bell, G.A. and Panhuber, H., Human psychophysics and 2-DG reveal how and where suppression with odor mixtures occur, *Am. Chemosens. Soc.*, VII, Abstract 114, (1985).
- 65 Lancet, D., Greer, C.A., Kauer, J.S. and Shepherd, G.M., Mapping of odor-related neuronal activity in the olfactory bulb by high-resolution 2-deoxyglucose autoradiography, *Proc. Natl. Acad. Sci. U.S.A.*, 79 (1982) 670–674.
- 66 LeGros Clark, W.E., Inquiries into the anatomical basis of olfactory discrimination, *Proc. R. Soc. (London) Ser. B*, 146 (1957) 299–319.
- 67 Lettvin, J.Y. and Gesteland, R.C., Speculation on smell, *Cold Spring Harbor Symp. Quant. Biol.*, 30 (1965) 217–225.
- 68 Leung, S.L.W., Model of gradual phase shift of theta rhythm in the rat, *J. Neurophysiol.*, 52 (1984) 1051–1065.
- 69 Lilly, J.C. and Cherry, R.B., Surface movements of figures in spontaneous activity of anesthetized cortex: leading and trailing edges, *J. Neurophysiol.*, 18 (1955) 18–32.
- 70 Livanov, M.N., *Spatial Organization of Cerebral Processes*, Wiley, New York, 1977, 181 pp.
- 71 Lopes da Silva, F.H., van Rotterdam, A., Storm van Leeuwen, W. and Tielen, A.M., Dynamic characteristics of visual evoked potentials in the dog. II. Beta frequency selectivity in evoked potentials and background activity, *Electroencephalogr. Clin. Neurophysiol.*, 29 (1970) 260–268.
- 72 MacKay-Sims, A., Shaman, P. and Moulton, D.G., Topographic coding of olfactory quality; odorant-specific patterns of epithelial responsivity in the salamander, *J. Neurophysiol.*, 48 (1982) 584–596.
- 73 Macrides, F. and Chorover, S.L., Olfactory bulb units: activity correlated with inhalation cycles and odor quality, *Science*, 175 (1972) 84–87.
- 74 Macrides, F., Eichenbaum, H.B. and Forbes, W.B., Temporal relationships between sniffing and the limbic theta rhythm during odor discrimination reversal learning, *J. Neurosci.*, 2 (1982) 1705–1717.
- 75 Mair, R.G., Response properties of rat olfactory bulb neurones, *J. Physiol. (London)*, 326 (1982) 341–359.
- 76 Martinez, D.M. and Freeman, W.J., Periglomerular cell action in mitral cells in olfactory bulb as shown by current source density analysis, *Brain Res.*, 308 (1984) 223–233.
- 77 Mathews, D.F., Response patterns of single units in the olfactory bulb of the rat to odor, *Brain Res.*, 47 (1972) 389–400.
- 78 Meisami, E. and Emami, S., Cytoarchitectural diversity in the main olfactory bulb: are there olfactory foveae?, *Am. Chemosens. Soc.* VII, Abstract, 130, 1985.
- 79 Moulton, D.G., Spatial patterning of response to odors in the peripheral olfactory system, *Physiol. Rev.*, 56 (1976) 578–593.
- 80 Moulton, D.G., Turk, A. and Johnson, J.W., Jr. (Eds.), *Methods in Olfactory Research*, Academic, New York, 1985, 386 pp.
- 81 Motokizawa, F. and Ino, Y., A search for olfactory receiving areas in the cerebral cortex of cats, *Neuroscience*, 6 (1981) 39–46.
- 82 Mozell, M.M., Olfactory discrimination: electrophysiological spatiotemporal basis, *Science*, 143 (1964) 1336–1337.
- 83 Mozell, M.M. and Jagdowicz, M., Chromatographic separation of odorants by the nose: retention times measured across in vivo olfactory mucosa, *Science*, 191 (1973) 1247–1249.
- 84 Nemitz, J.W. and Goldberg, S.J., Neuronal responses of rat pyriform cortex to odor stimulation: an extracellular and intracellular study, *J. Neurophysiol.*, 49 (1983) 188–203.
- 85 Nicoll, R.A., Recurrent excitation of secondary olfactory neurons: a possible mechanism for signal amplification, *Science*, 171 (1971) 824–825.
- 86 Nunez, P.L., *Electric Fields of the Brain*, Oxford Univ. Press, New York, 1981, 484 pp.
- 87 O'Keefe, J. and Nadel, L., *The Hippocampus as a Cognitive Map*, Oxford, Clarendon, 1978, 570 pp.
- 88 Palm, G., Neural assemblies: an alternative approach to artificial intelligence, *Studies in Brain Function*, Vol. 7, Springer-Verlag, New York, 1982, 244 pp.
- 89 Plonsey, R., *Bioelectric Phenomena*, McGraw-Hill, New York, 1969, 380 pp.
- 90 Potter, H. and Chorover, S.L., Response plasticity in hamster olfactory bulb: peripheral and central processes, *Brain Res.*, 116 (1976) 419–429.
- 91 Rall, W. and Shepherd, G.M., Theoretical reconstruction of field potentials and dendrodendritic synaptic interactions in olfactory bulb, *J. Neurophysiol.*, 31 (1968) 884–915.
- 92 Schoenfeld, T.A., Marchand, J.E. and Macrides, F., Topographic organization of tufted cell axonal projections in the hamster main olfactory bulb: an intrabulbar association system, *J. Comp. Neurol.*, 235 (1985) 503–518.
- 93 Seyal, M., *A Neuropharmacological Study of Evoked Potentials in the Olfactory Bulb*, Ph.D. Thesis, University of California, Berkeley, 1976.
- 94 Sharp, F.R., Kauer, J. and Shepherd, G.M., Laminar analysis of 2-deoxyglucose uptake in olfactory bulb and olfactory cortex of rabbit and rat, *J. Neurophysiol.*, 40 (1977) 800–813.
- 95 Sheer, D., Focused and arousal 40-Hz EEG, In R.M. Knights and D.J. Baker (Eds.), *The Neuropsychology of Learning Disorders: Theoretical Approaches*, Baltimore, MD, University Park Press, 1976, pp. 71–87.
- 96 Sherrington, C.S., Some functional problems attaching to convergence, *Proc. R. Soc. London Ser. B*, 105 (1929)

- 332-362.
- 97 Skarda, C.A., Explaining behavior: bringing the brain back in, *Inquiry*, in press.
- 98 Skeen, L.C., Odor-induced patterns of deoxyglucose consumption in the olfactory bulb of the tree shrew (*Tupaia glis*), *Brain Res.*, 124 (1977) 147-153.
- 99 Stewart, W.S., Kauer, J.S. and Shepherd, G.M., Functional organization of rat olfactory bulb analyzed by the 2-deoxyglucose method, *J. Comp. Neurol.*, 185 (1979) 715-734.
- 100 Tanabe, T., Iino, M. and Takagi, S.F., Discrimination of odors in olfactory bulb, pyriform-amygdaloid areas and orbitofrontal cortex of the monkey, *J. Neurophysiol.*, 38 (1975) 1284-1296.
- 101 Thatcher, R.W. and John, E.R., *Functional Neuroscience, Vol. I. Foundations of Cognitive Processes*, Hillsdale, N.J., Lawrence Erlbaum, Assoc., 1977, 382 pp.
- 102 Thommesen, G., The spatial distribution of odor-induced potentials in the olfactory bulb of char and trout (*Salmonidae*), *Acta Physiol. Scand.*, 102 (1978) 205-217.
- 103 Tolman, E.C., Cognitive maps in rats and men, *Psychol. Rev.*, 55 (1948) 189-208.
- 104 Viana Di Prisco, G., Hebb synaptic plasticity, *Progr. Neurobiol.*, 22 (1984) 89-102.
- 105 Viana Di Prisco, G. and Freeman, W.J., Odor-related bulbar EEG spatial pattern analysis during appetitive conditioning in rabbits, *Behav. Neurosci.*, 99 (1985) 964-978.
- 106 Willey, T.J., The ultrastructure of the cat olfactory bulb, *J. Comp. Neurol.*, 152 (1973) 211-232.
- 107 Walter, W.G., *The Living Brain*, Norton, New York, 1953, 311 pp.
- 108 Williams, H. and Nottebohm, F., Auditory responses in avian vocal motor neurons: a motor theory for song perception in birds, *Science*, 229 (1985) 279-282.
- 109 Yamaguchi, K. and Ueda, K., Rhythmic discharge of mitral cells in the carp olfactory bulb, *Brain Res.*, 322 (1984) 378-381.